



Project no.: **NMP3-CT-2005-013644**

Project acronym: **MULTIMATDSIGN**

**Computer aided molecular design of multifunctional materials with controlled permeability properties**

Instrument: **STREP**

Thematic Priority: **NMP**

**Publishable final activity report**

Period covered: from March 1<sup>st</sup>, 05 to February 28th, 08 Date of preparation: April 20<sup>th</sup>, 08

Start date of project: March 1<sup>st</sup>, 05

Duration: 36 Months

Project coordinator name: Prof. Dr. Dieter Hofmann

Project coordinator organisation name: GKSS

Revision [draft 1]

## 1. Project execution

### 1.1 Project objectives

Many important processes in chemical industry, biotechnology, biomedical engineering and other fields depend critically on the transport of small and medium sized molecules (e.g. oxygen, water, ethanol, benzene etc.) through polymer based materials (e.g. used for permselective membranes, packaging materials, highly oxygen permeable contact lenses or drug release systems). These materials are typically multifunctional combining appropriate transport properties with other features like biocompatibility, biodegradability, mechanic strength or catalytic activity.

The properties of these materials with regard to transport of small and medium sized molecules typically depend on structural features of the utilised materials on multiple length and time scales. This starts on the level of the arrangement of individual atoms (sub- and low nanometre scale) which e.g. determines the free volume needed for any kind of molecular transport. If e.g. copolymers or polymer blends are used homopolymer domains may be formed with radii on the higher nanometre to low micrometer scale. If composites from polymers with inorganic fillers are applied even longer length scales may be of relevance.

Hitherto the development of polymer based materials for the solution of specific molecular transport problems was mainly based on experimentation including trial and error concepts and correlative thinking. This traditional approach can be quite laborious and resource consuming. Over the last 20 years however the foundations have been laid to now support materials research and development by systematic multi scale computer aided molecular design (CAMD). This shall lead to a much more efficient knowledge-based approach.

Based on the foregoing remarks the main aims of this project are multidisciplinary efforts using advanced computational tools of materials modelling for the understanding and knowledge-based design of multi-functional polymeric materials which combine controlled permeability to selected small molecules with various other properties needed to ensure processability, durability and multiple end-uses. This aim is pursued by the development and extensive application of multiscale computer-aided material modelling and design methodology, complemented by computer-assisted evaluation of end-use performance of the materials in question. Simulation results will be validated against experimental data. Wherever possible, measures will be taken to demonstrate the applicability of design projects in actual product and process design.

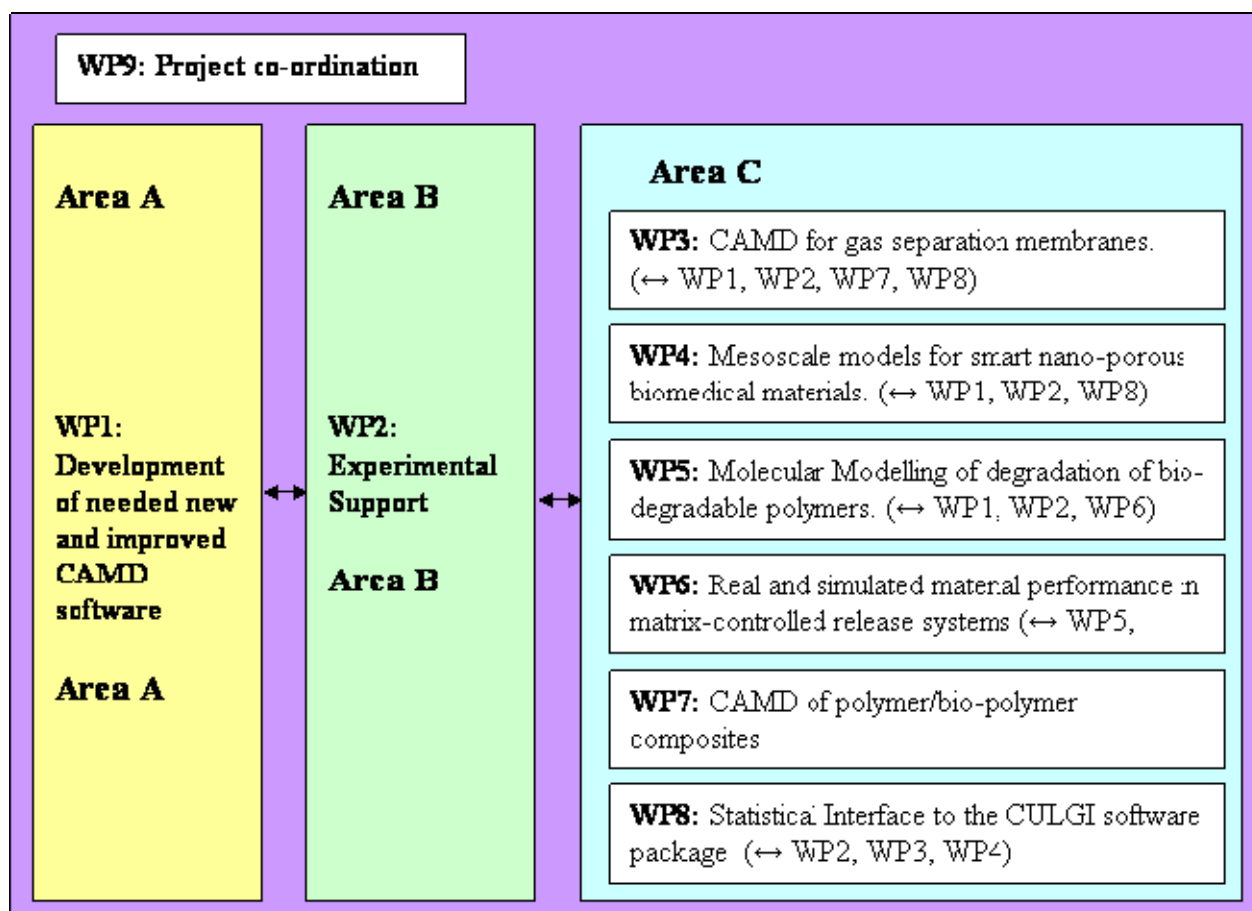
The main idea of the MULTIMATDESIGN workplan is to combine efforts of leading European CAMD software developers/providers, experimentalists and users of CAMD and other modelling software to demonstrate that breakthrough solutions are possible for the design of multifunctional materials with key permeability related properties. For this purpose workpackages (WP) in three highly interlinked areas are defined. These are:

**Area A:** While there are already a number of software tools available for CAMD activities on different length scale, there is still a need for the development of new and/or improved CAMD methodology. This mainly applies to the fields of Monte Carlo (MC) methods, force field-based molecular mechanics (MM), Transition state (TST) methodology, mesoscale methods and finite element (FE) or finite difference techniques. These activities will e.g. lead to a new tool for the simulation of sorption isotherms using atomistic bulk models. In addition an artificial intelligence approach will be developed, to most efficiently utilise large sets of experimental and simulation data for design purposes.

**Area B:** CAMD approaches only make sense in the context of related experimental work to either validate simulation data or to confirm CAMD predictions. Therefore, actual synthesis, and/or sample formation and experimental characterisation of polymer based materials relevant for the project are planned.

**Area C:** The major activity of MULTIMATDESIGN consists in CAMD applications demonstrating the very substantial and broad potential of this modern knowledge-based approach for decisive contributions to breakthrough solutions for a range of permeability related problems by material design complemented with computer-aided evaluation of end-use performance of the relevant material. The areas of CAMD application are briefly mentioned in the scheme below.

The interrelation between the activities in the different areas is as follows. Area A needs specific basic validation, i.e. comparison with experimental data, which are obtained from Area B. Area A results also need to be proven in real life applications before successful new tools can be marketed. This is performed in Area C which in turn profits from the improvements of the available CAMD and other related modelling methodology coming from Area A. In addition Area C activities in most cases lead to actual design projects followed by "real" experimental activity (i.e., synthesis, sample formation, characterisation) which is mostly done again in Area B. Also the individual workpackages of Area C are interlinked in many ways (cf. below).



## 1.2 Contractors

Participant name	Participant short name	Country	Contact person
GKSS Forschungszentrum Geesthacht GmbH, Teltow	<a href="#">GKSS</a>	Germany	<a href="#">Dieter Hofmann</a>
National Research Centre for the Physical Sciences “Demokritos”, Athens	<a href="#">Demokritos</a>	Greece	<a href="#">Doros N. Theodorou</a>
L' Air Liquide S.A, Paris	<a href="#">Air Liquide</a>	France	<a href="#">Pluton Pullumbi</a>
Research Institute on Membrane Technology, Rende	<a href="#">ITM-CNR</a>	Italy	<a href="#">Elena Tocci</a>
Accelrys Ltd., Cambridge	<a href="#">Accelrys</a>	United Kingdom	<a href="#">Stephen Todd</a>
Universiteit Leiden	<a href="#">Leidenuniv</a>	The Netherlands	<a href="#">Alexander Kros</a>
MatSim GmbH, Zurich	<a href="#">MatSim</a>	Switzerland	<a href="#">Olga Guseva</a>
A.V. Topchiev Institute of Petrochemical Synthesis, Moscow,	<a href="#">TIPS</a>	Russia	<a href="#">Yuri Yampolski</a>
Politecnico di Milano	<a href="#">Polimi</a>	Italy	<a href="#">Franco Montevercchi</a>
Alma Mater Studiorum - Università di Bologna	<a href="#">UNIBO</a>	Italy	<a href="#">Giulio Sarti</a>
Mesodyn BV Oegstgeest	<a href="#">Mesodyn</a>	The Netherlands	<a href="#">Johannes G.E.M. Fraaije</a>

## 1.3 co-ordinator contact details and project public website

Prof. Dr. Dieter Hofmann  
GKSS-Research Center, Institute of Polymer Research  
Kantstr. 55, D-14513 Teltow  
Tel. +49 3328 352 247  
Fax. +49 3328 352 452  
hofmann@gkss.de,  
<http://www.gkss.de>

[Multimatdesign.gkss.de](http://Multimatdesign.gkss.de)

## 1.4 work performed, results achieved, intentions for use and impact.

**Work package 1 (WP 1) “Development of new and improved CAMD software“:** New software for permeability property prediction will be developed. Based on a critical assessment of the state of the art, mainly improvements of existing atomistic-, mesoscale- and continuum methodology will be pursued, including for example improved Monte Carlo (MC) and other atomistic simulation techniques as well as a new finite element (FE) technique for property prediction of arbitrary structured multiphase morphologies with diffusive interfaces.

**Goals:** Generation of realistic atomistic configurations for glassy polymers consisting of repeat units with complex chemical constitution via coarse-graining – equilibration – reverse mapping strategies. Computation of entire sorption isotherms of gases in glassy polymers, up

to high penetrant activities. Calculation of penetrant diffusivities in glassy polymer matrices via multidimensional Transition State Theory (TST)-based strategies.

**Coarse-graining -Equilibration- Reverse mapping:** The first objective was to generate realistic atomistic configurations of **polystyrene (PS)**, a polymer with high practical interest. A new coarse-graining (CG) model suitable for vinyl polymers was developed and tested on PS. The new model is able to keep information on stereochemical sequences and it was parameterized by means of the Iterative Boltzmann Inversion method (IBM) developed in the group of Müller-Plathe. The new model was applied on PS melts of different chain lengths. The equilibration of high molecular weight melts (up to 210000 g/mol) was achieved via the connectivity-altering Monte Carlo algorithms designed in our group. Long range conformational properties, like radius of gyration ( $R_g$ ) (Figure 1 (left)) and end-to-end distance ( $R$ ) were derived in good agreement with experimental data. Accordingly, the chain stiffness was also predicted satisfactorily (Figure 1 (right)).

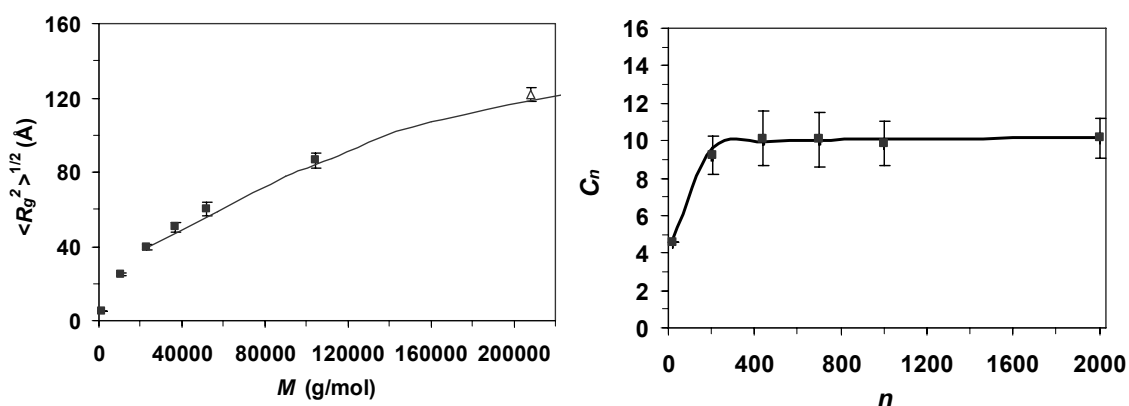


**Figure 1.** (left) Average radius of gyration of the coarse-grained chains as a function of molar mass  $M$  in the melt at 500 K (filled symbols). With the open symbol is shown the result for the 2000-mer chains at a different temperature (413 K). The continuous line is neutron-scattering results for high molar mass a-PS in the bulk. (right) Characteristic ratio of the coarse-grained chains as a function of chain length  $n$  at 500 K. The drawn line indicates the plateau at a value of approximately 10.

Topological analysis of entanglements with the Tzoumanekas and Theodorou approach (*Macromolecules*, **2006**, 39, 4592) on high MW melts produced very satisfactory results for the entanglement molecular weight ( $M_e$ ), the packing length ( $p$ ), and the reptation tube diameter ( $d$ ).

The equilibrated coarse-grained system was subsequently mapped onto an atomistic one by implementing a reverse mapping strategy which proceeds by generating first an initial guess of the atomistic structure in a purely geometrical fashion, and then minimize progressively with respect to its intra- and intermolecular energy by using a Monte Carlo method comprising mainly flip moves. Final relaxation is achieved via short-time canonical molecular dynamics simulation. The atomistic configurations, thus generated, yielded structural properties, i.e. structure factor  $S(k)$  in good agreement with X-ray measurements (Figure 2). The excellent agreement between the short chain and the reverse-mapped system indicates that the discrepancies observed with respect to the experimental data, mainly the  $q$  at which the polymerization peak appears and the relative height of the two first peaks, are due to the force field and not to insufficient equilibration.

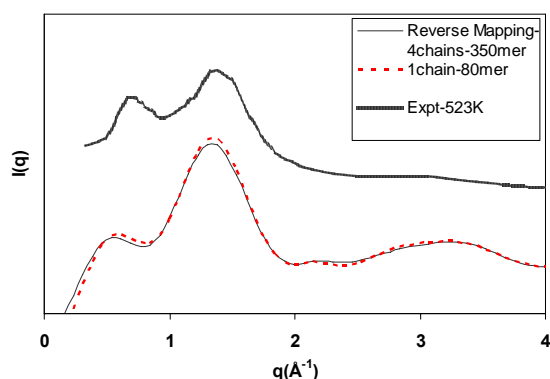


**Figure 2.** Calculated scattering intensity from a melt of reverse-mapped chains of 350mers at 500 K (continuous line) and from a small model melt system constructed from a single 80-mer parent chain at the same  $T$  (dotted line). Over the simulation results, with the thick dotted line, is shown the experimental X-ray scattering pattern of atactic PS at 523 K.

**Sorption isotherms:** A strategy allowing the computation of sorption isotherms, up to high penetrant activities, in glassy matrices has been designed. Glassy matrices of PS obtained from reverse mapping are loaded with  $\text{CO}_2$  at various compositions by mapping the accessible free volume. The new scheme permits an equilibrium repartition of  $\text{CO}_2$  in the thermally fluctuating polymer matrix, simulated via molecular dynamics. The scheme is coupled with an efficient methodology for the calculation of the penetrant fugacity, i.e. the Direct Particle Deletion method, a generalization of the Staged Particle Deletion method (Boulougouris et al., *Mol. Phys.* **1999**, 96, 905). The sorption isotherms of  $\text{CO}_2$  in PS and the induced polymer swelling have been calculated in the temperature range from 308 K to 405 K (below and above the glass transition temperature of the pure polymer) and for pressures up to 300 bar. In Figures 3 and 4, the simulation results are compared with experimental data for the sorption and swelling of the  $\text{CO}_2$ /PS system at a low (308 K) and a high temperature (373 K). The comparison is very satisfactory at low  $T$  for pressures below 50 bar and at high  $T$  in the entire pressure range. At low  $T$  the polymer saturates at a lower concentration compared to the recent results of Panayiotou and collaborators (refs [1] and [2] of Figure 4). The quality of the glass (history of formation, free volume distribution etc), the molecular model and/or the long relaxation times of the polymer can be in the origin of these discrepancies. In any case, the experimental data themselves show a large scatter at low temperatures and high pressures.

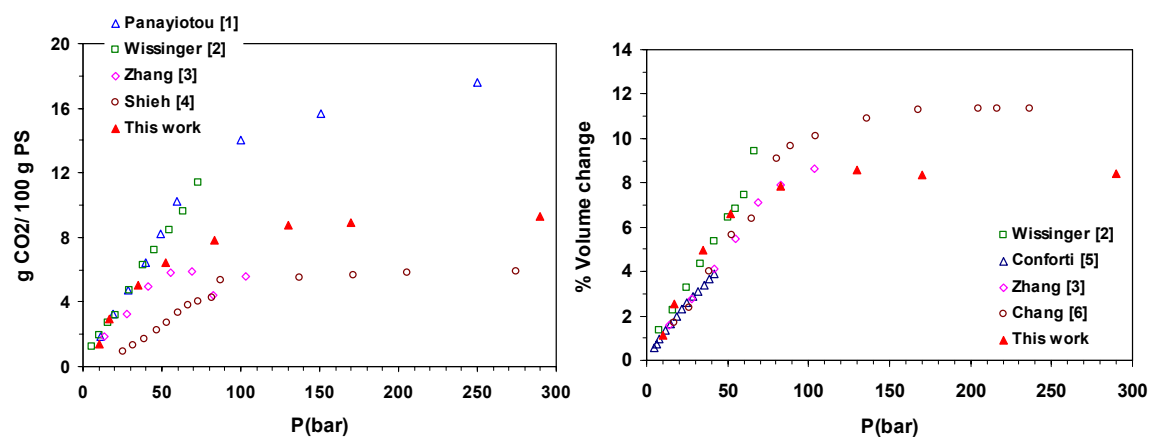


**Figure 3.** Comparison of simulation results and experimental data for the sorption of  $\text{CO}_2$  in PS and the induced swelling at  $T=308$  K and for pressures up to 300 bar. [1]: *J. Supercrit. Fluids* **2006**, 37, 254, [2]: *J. Polym. Sci. B: Polym. Phys.* **1987**, 25, 2497, [3]: *J. Supercrit. Fluids* **1997**, 11, 115, [4]: *J. Supercrit. Fluids* **2003**, 25, 261, [5]: *Macromolecules* **1996**, 29, 6629, [6]: *J. Supercrit. Fluids* **1998**, 13, 113.

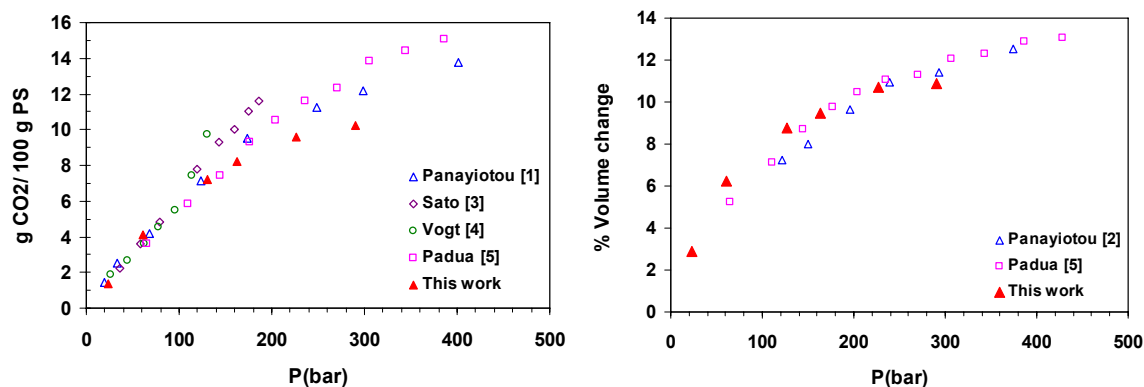


**Figure 4.** Comparison of simulation results and experimental data for the sorption of CO<sub>2</sub> in PS and the induced swelling at  $T=373$  K and for pressures up to 300 bar. [1]: *J. Supercrit. Fluids* **2006**, 37, 254, [2]: *J. Supercrit. Fluids* **2007**, 39, 426, [3]: *Fluid Phase Equilib.* **1996**, 125, 129, [4]: *Macromolecules* **2003**, 36, 4029, [5]: *J. Polym. Sci. B: Polym. Phys.* **2001**, 39, 2063.

Time autocorrelation functions have been computed for the pendant CH(al)-C(ar) bond of PS at each temperature as a function of pressure. Predicted correlation times ( $\tau$ ) are used in order to locate the glass transition pressure ( $P_g$ ) at each temperature, by setting  $\tau = 100$ s, and the results compare well with experimental data. Derivative properties, such as the partial molar volume and the partial molar enthalpy of CO<sub>2</sub> have been calculated in good agreement with experimental findings.

**Multidimensional TST for calculating permeability in a glassy matrix:** The diffusivity of CO<sub>2</sub> in a glassy configuration of poly(amide imide) (PAI) has been calculated, using the new multidimensional TST tool and the COMPASS force field. A kinetic Monte Carlo (KMC) scheme was employed for the calculation of diffusivity of CO<sub>2</sub> in the structure of PAI. The KMC simulation was conducted in a macrostate network formed by periodic replication of the amorphous cell used to simulate the polymer. The network used was dictated by the determination of the reaction paths and the calculated rate constants. The network nodes represent the centers of the macrostates and the bonds (connections) between the nodes are established along nonzero values of transition rate constants. A large number of random walkers were distributed on the network nodes according to equilibrium occupancy probabilities, which were calculated using Widom test insertion method within each macrostate. The diffusivity was estimated from the mean square displacement computed over all random walkers through the Einstein equation. The diffusion coefficient was calculated as  $0.25 \times 10^{-8} \text{ cm}^2 \text{ s}^{-1}$  [experimental value:  $0.81 \times 10^{-8} \text{ cm}^2 \text{ s}^{-1}$ , Fritsch and Peinmann, *J. Memb. Sci.*, **1995**, 99, 29].

The solubility of CO<sub>2</sub> in PAI was calculated using the Widom test particle insertion method in a fluctuating polymer structure. The solubility coefficient was calculated equal to  $0.42 \text{ cm}^3 \text{ (STP)} / (\text{cm}^3 \text{ polymer cmHg})$ .

The permeability was estimated as the product of the solubility and diffusivity coefficient equal to  $10.5 \text{ cm}^3 \text{ (STP) cm} / \text{cm}^2 \text{ s cmHg} \times 10^{-10}$  (barrer). [experimental values: a)  $9.54 \text{ cm}^3 \text{ (STP) cm} / \text{cm}^2 \text{ cmHg} \times 10^{-10}$  (barrer), Fritsch and Peinmann, *J. Memb. Sci.*, **1995**, 99, 29, and b)  $15.01 \text{ cm}^3 \text{ (STP) cm} / \text{cm}^2 \text{ cmHg} \times 10^{-10}$  (barrer), Nagel et al., *Macromolecules*, **2002**, 35, 2071].

In an additional activity a new grid based FE technology for predicting the overall permeability properties of arbitrary structured complex multiphase morphologies with diffusive interfaces was developed and implemented in the commercial product Gridder at MatSim. A commercial version of Gridder with the capability for predicting the overall

thermo-elastic properties of multiphase materials with nearly incompressible phases (rubbers, hydrogels, etc.) is now available at MatSim.

## **WP2 “Experimental Support”:**

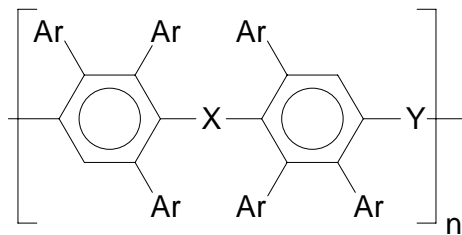
Contribution of TIPS (Tasks 2.1-2.3)

Creation and characterization of novel polymeric materials for development of advanced design of materials for separation of gases and vapors.

Task 2.1. An interesting group of prospected membrane materials – poly(phenylenephenylenes) will be studied; after determination of the transport parameters (P,D,S) and free volume they would be suggested as potential objects of computer modelling.

Description of background and key results

The incentive for selection of this group of polymers was an interest to them because of low electrical permittivity  $\epsilon$  (so-called low-k polymers), potential materials for electronic industry. This property of polymers often correlates with large free volume and, hence, high gas permeability. Several polymers of a general formula



where Ar is phenyl and X and Y are aromatic moieties, were tested. An unexpected result was a discovery of unusually high permselectivity in respect of carbon dioxide. Nearly all the polymers prepared and studied showed the data points at the Robeson diagrams for the pair  $\text{CO}_2/\text{N}_2$  and  $\text{CO}_2/\text{CH}_4$  above the upper bound.

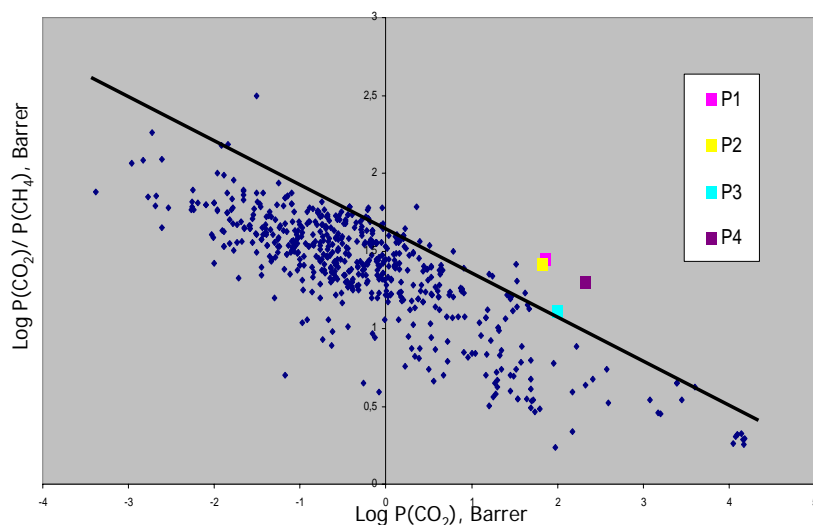
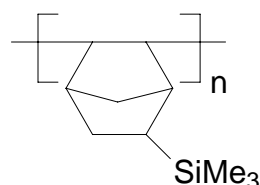


Fig.1. TIPS Robeson diagram for carbon dioxide – methane pair.

In order to explain this behaviour we undertook quantum chemical calculations of the interactions between CO<sub>2</sub> and model low molecular mass aromatic compounds. It was shown that carbon dioxide reveal relatively high (36-46 kJ/mol) interactions with aromatic rings in such compounds as biphenyl; *p*- and *m*-biphenylbenzenes, 1,2,4-triphenylbenzene, terphenyls. The interactions take place at large distances (3-3.5 Å). Such polymers with great concentration of aromatic structures can form a basis for membrane materials for extraction of carbon dioxide from various gas mixtures, and important task for environmental protection. Another study of the same Task was focused on a novel high free volume, highly permeable polymer – addition type poly(trimethylsilyl norbornene).



This polymer was distinguished by great permeability coefficients for gases:

Table 1. Transport parameters of the addition type Si-substituted polynorbornene

Gas	Permeability coefficient, Barrer
He	790
H <sub>2</sub>	1680
O <sub>2</sub>	780
N <sub>2</sub>	297
CO <sub>2</sub>	4350
CH <sub>4</sub>	790
C <sub>2</sub> H <sub>6</sub>	1430
C <sub>3</sub> H <sub>8</sub>	1740
C <sub>4</sub> H <sub>10</sub>	17500

Especially interesting was an observation that the permeability coefficients of hydrocarbons (at 1 atm) increase when the size of the penetrants increases (see table).

According to the results of positron annihilation lifetime study, this polymers is characterized by long lifetimes, i.e. large sizes of free volume element, that are independent of temperature, another peculiarity of highly permeable polymers. Low activation energies of permeation (in some cases negative) manifest low energy barriers of diffusion and are in line with observed solubility controlled permeation (see the data for hydrocarbons in Table).

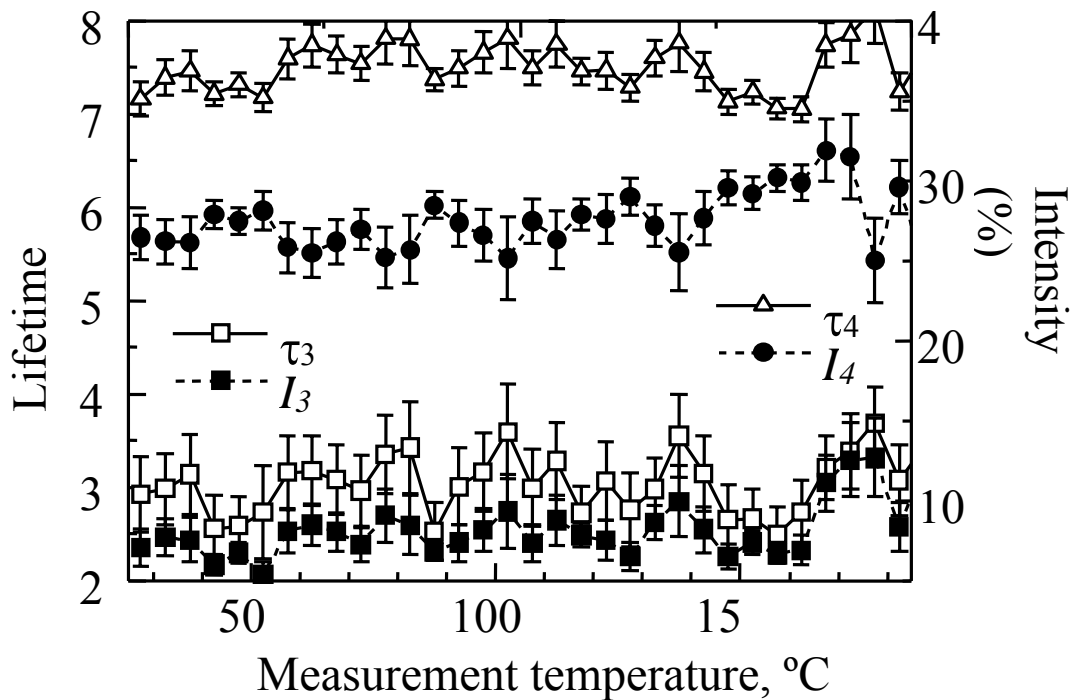


Fig. 2. Temperature dependence of lifetimes and intensity in addition type PTMSN

The size of free volume element in this polymer (according PALS) is about  $775 \text{ \AA}^3$ , what is consistent with the results of the determination of this values using the inverse gas chromatography (IGC).

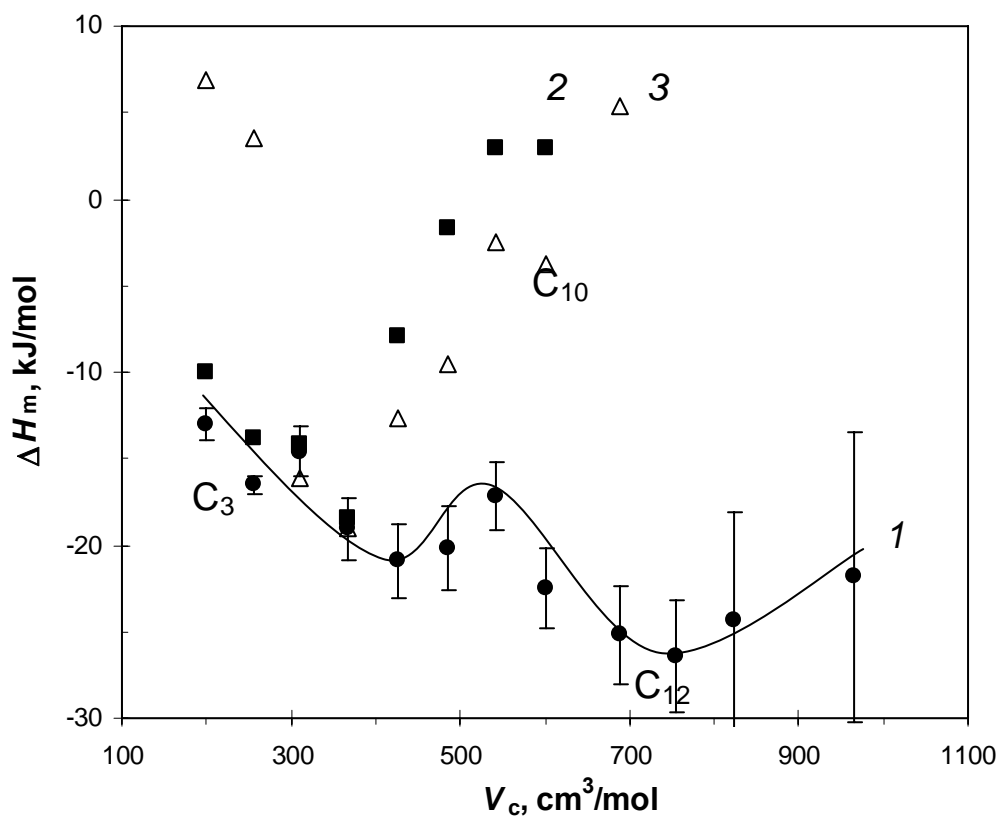


Fig. 3. Partial molar enthalpy of mixing versus the critical volume of solutes (n-alkanes). The coordinates of the minima correspond to the size of free volume element.

It is seen that the size of free volume element in this polymer is larger than those in poly(vinyltrimethylsilane) (2, PVTMS) and amorphous Teflon AF1600 (3). The IGC studies also indicated that this polymers has very large solubility coefficients, similar to those of poly(trimethylsilyl propyne).

By and large, this polymer is a suitable material for membrane separation of light gases and, especially, separation of heavier hydrocarbons from natural and associated petroleum gases (the latter was confirmed by a patent granted to TIPS).

Task 2.2. The experimental work will include a study of novel polyimides (PI), objects of computer modelling in WP3: determination of the gas permeability (P), diffusion (D) and solubility (S) coefficients.

Scope of activity: In total, 12 polyimides, copolyimides and polyetherimides of different structure were studied. Permeability, diffusion and solubility coefficients for standard set of gases (H<sub>2</sub>, O<sub>2</sub>, N<sub>2</sub>, CO, CO<sub>2</sub>, CH<sub>4</sub>) were determined.

The most interesting results were obtained during the studies of the transport properties of poly(etherimides) (PEI). In this investigation, a novel principle of the control of selectivity of gas separation due to conditioning in strained state of the polymer films containing residual solvent that is capable for hydrogen bonding. With a very good reproducibility, it was demonstrated that very selective “state” of polymer films can be obtained if removal of solvent (e.g. chloroform) is performed from films mechanically restricted, as Fig. 4 illustrates. Quantum chemical calculations and FTIR studies indicated that the sites responsible for H-bonding in PEIs are ether bonds (Ph-O-Ph).

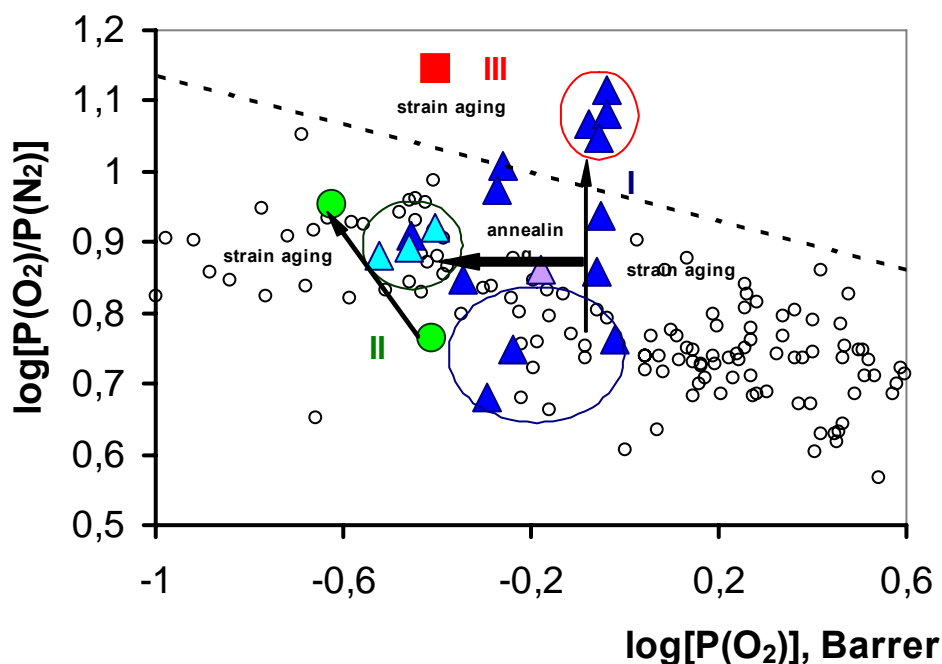


Fig.4. Robeson diagram for O<sub>2</sub>/N<sub>2</sub> pair: strain aged polymers give highly selective film if the solvent (e.g. CHCl<sub>3</sub>) can form H-bonds; DHF as a solvent does not results in this effect;

annealing in free state also lead to less permselective films (I, II and III – polyetherimides with different structure).

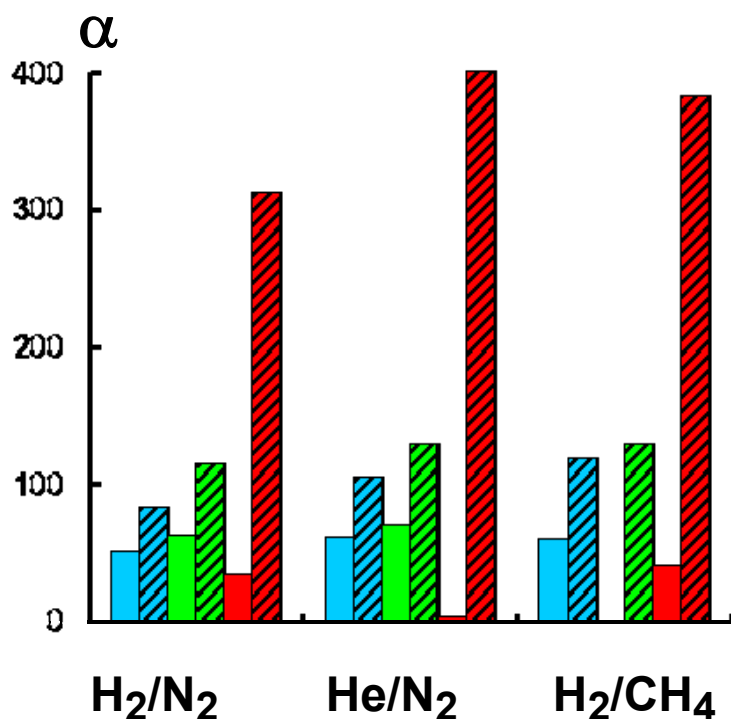


Fig.5. Separation factors of 3 different PEI: left bars are for standard solvent treatment, right (striped) bars are for “strain aged” samples.

This principle of control of gas permeation properties of polymers are now being studied using polymers of other classes and other low molecular mass compounds. It can be claimed that this idea expands classical QSAR approach for selection of the best membrane materials basing on chemical structure of polymers.

Works published:

1. Vidyakin M., Lazareva Yu., Yampolskii Yu., Alentiev A., Ronova I., A., Bruma M., Hamciuc E., Lungu R. Transport properties of polyimides with phenylhinoxalene fragments, *Vysokomol. Soed.*, 2007, A, 49, 1703.
2. Vidyakin M., Lazareva Yu., Alentiev A., Rusov D., Yampolskii Yu., Ronova I., Keshtov M., Transport properties of polyphenylhinoxalenes with heterocycl fragments *Vysokomol. Soed.*, 2007, B, 49, 1878.
3. Yu. Yampolskii, Methods for investigation of free volume in polymers, *Russ. Chem. Rev.*, 2007, 76, 59.
4. Yu.Kostina, G.Bondarenko, A.Alentiev, Yu.Yampolskii, Effects of the structure and conformation set on the transport parameters of polyetherimides, *Vysokomol. Soed.*, 2007, A, 49, 96.
5. E.Finkelshtein, K.Makovetskii, M.Gringolts, Yu.Rogan, T.Golenko, L.Starannikova, Yu.Yampolskii, V.Shantarovich, T.Suzuki, Addition-type polynorborene with Si(CH<sub>3</sub>)<sub>3</sub> side group: synthesis, gas permeation and free volume, *Macromolecules*, 39, 7022 (2006).

Work submitted:

L.Starannikova, M.Pilipenko, N.Belov, Yu.Yampolskii\*, M.Gringolts, E.Finkelshtein, Addition-type polynorbornene with Si(CH<sub>3</sub>)<sub>3</sub> side groups: detailed study of gas permeation and thermodynamic properties, J.Membr.Sci.

Patent:

E.Finkelshtein, K.Makovetskii, M.Gringolts, Yu.Rogan, T.Golenko, Yu.Yampolskii, L.Starannikova, N.Plate, Addition type poly(5-trimethylsilylnorborn-en) and the process of gas separation using the membranes based on it, Patent RF, 2 296 773, 2007.

**Task 2.4:** Experimental characterisation of the influence of solvent type, film casting and drying, and membrane thermal treatment on permeability (solubility, diffusivity) of membranes of glassy perfluorinated copolymers (Hyflon of Ausimont) in WP 3 for permanent gases and/or vapours. Stabilisation of 'universal' criteria for membrane preparation and pre-measurement treatment. Determination of the gas permeability (P), diffusion (D) and solubility (S) coefficients, for rubbery polyamide copolymers in WP 7.

#### **Description of background and key results**

Like other amorphous glassy perfluoropolymers, Hyflon AD is highly permeable to permanent gases, offering interesting perspectives for its use in gas separation membranes, especially because of its high thermal, chemical, ageing and weather resistance and excellent inertness to most organic solvents. The preparation and gas transport properties of Hyflon membranes has been subject of extensive studies [1,2,4].

In order get a better understanding of the polymer properties which determine the transport phenomena that were studied extensively, a method was developed to evaluate the size distribution of free volume elements in Hyflon AD membranes by photochromic probes. First a method for effective dispersion of the probes in the polymer matrix and for their successive light-induced isomerisation was developed. Then it was shown that for two grades of Hyflon AD (60X and 80X) the cumulative free volume distribution curve has a typical sigmoidal shape, and that Hyflon AD80X has somewhat larger free volume elements than Hyflon AD60X. The procedure for the determination of the free volume size distribution in Hyflon AD membranes by the photochromic probe method has been elaborated during the extent of the project. In this method photo-isomerizable molecules, usually stilbenes and azobenzenes, are dispersed homogenously into the polymer matrix. Upon irradiation with UV or visible light the photochromic molecules undergo trans-cis isomerisation (Figure 1). This can only occur when a sufficient amount of free volume is available for the rotation of the molecule in the polymer matrix.

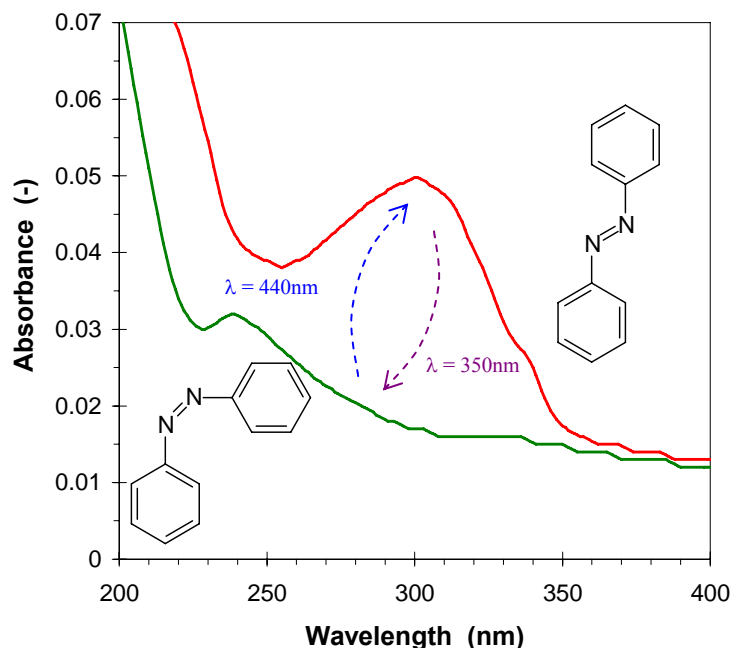


Figure 1. UV spectra of a Hyflon AD60X membrane containing 0.06 wt.-% of trans- and cis-azobenzene. Trans-cis isomerization occurs upon irradiation at 350 nm and the reverse reaction occurs at 440 nm.

Six membranes were prepared with different photochromic probe molecules. The ratio between the amount of cis isomer in the film and in solution after the irradiation was determined by UV spectroscopy. This ratio is a measure of the capability of the photochromic probe to isomerize in the polymer matrix and it indicates the availability of free volume elements of sufficiently large size. A plot of this ratio as a function of the total isomerisation volume (i.e. molar volume plus extra volume required for isomerization) yields the size distribution of free volume elements in the polymeric material (Figure 2).

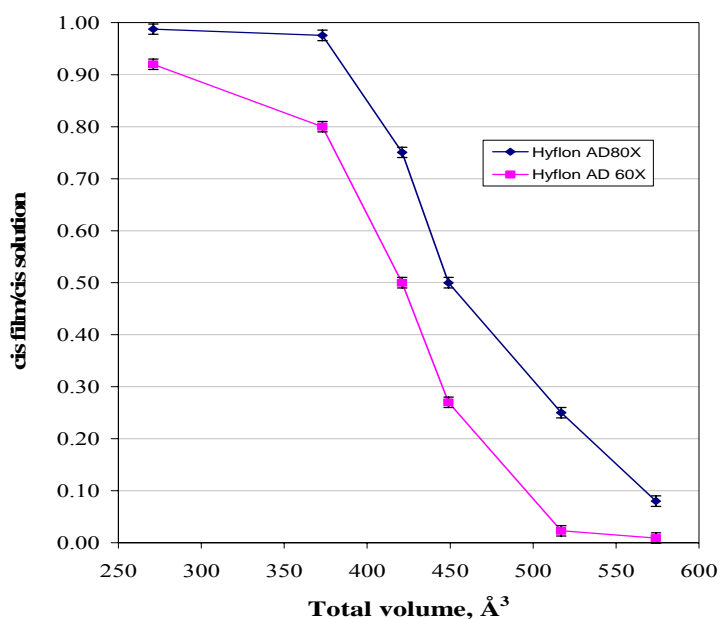


Figure 2. Ratio of the cis isomer in the film and the cis isomer in solution as a function of the total isomerisation volume in Hyflon AD.

It appears that nearly all free volume elements have a minimum size of about  $250\text{\AA}^3$ , whereas no free volume elements with dimensions larger than about  $600\text{\AA}^3$  exist. Furthermore, the entire size distribution of free volume elements in Hyflon AD80X is clearly shifted to higher volume compared to Hyflon AD60X. This is in agreement with the higher gas permeability usually observed in Hyflon AD80X.

The results are also in good agreement with preliminary PALS data of provided by TIPS, which indicate an average free volume size that lies inside the range covered by the curve obtained with the photochromic probe method for both grades of Hyflon.

In order to complete the characterization of gas transport properties single gas permeation experiments were carried out at 1 bar of feed pressure covering a broad range of temperature ( $25\text{-}85^\circ\text{C}$ ) in pure Pebax (for WP7). The permeability coefficients were evaluated for each single gas from the steady state values. Differently, the diffusivity of each one was estimated from three different diffusion coefficients [ $D_{1/2}$ ,  $D_{\text{slope}}$ ,  $D_{\square}$   $\text{cm}^2/\text{s}$ ] calculated at three different times of the transient state. An evaluation of the dependence of the transport on the temperature was made by calculating the activation energy for permeation and diffusivity according to the Arrhenius law. A non-linear behaviour in water sorption and membrane surface energies was observed as the content of an aromatic sulphonamide (KET) was increased. The macroscopic phenomenon of variation of the membrane affinity was first estimated by quantifying the difference of the solubility parameters between membranes and penetrants. In particular, the variations in surface free energy caused by a different availability and accessibility of specific functional groups of both the modifier and polymer segments were evaluated. Infrared analysis yielded indication about the accessibility and availability of free polar groups, enabling to form hydrogen-bonding with water. The amphiphilic KET structure produced remarkable modifications of the surface character of membranes. The membranes exhibited a gradual increase in hydrophilicity up to 50 wt.% of KET, whereas a dramatic reduction in wetting degree was appreciated at 70 wt.%. Contact angle experiments evidenced changes in the water droplet spreading on the different membrane surfaces, due to formation of attractive and/or repulsive intermolecular interactions between the probing water and the polymer surface (Figure 3a).

In Figure 3a, a clear maximum value of the  $\tilde{\sigma}$  ( $\text{mJ}/\text{m}^2$ ) was found in correspondence to the minimum of water contact angle at the 50%wt of KET. A dramatic decreased in  $\tilde{\sigma}$  ( $\text{mJ}/\text{m}^2$ ) followed, as the concentration of KET raised. This implies that the amount of the modifier polar moieties increased facilitating the membrane-water molecular interactions, as the concentration of modifier increased up to 50%.

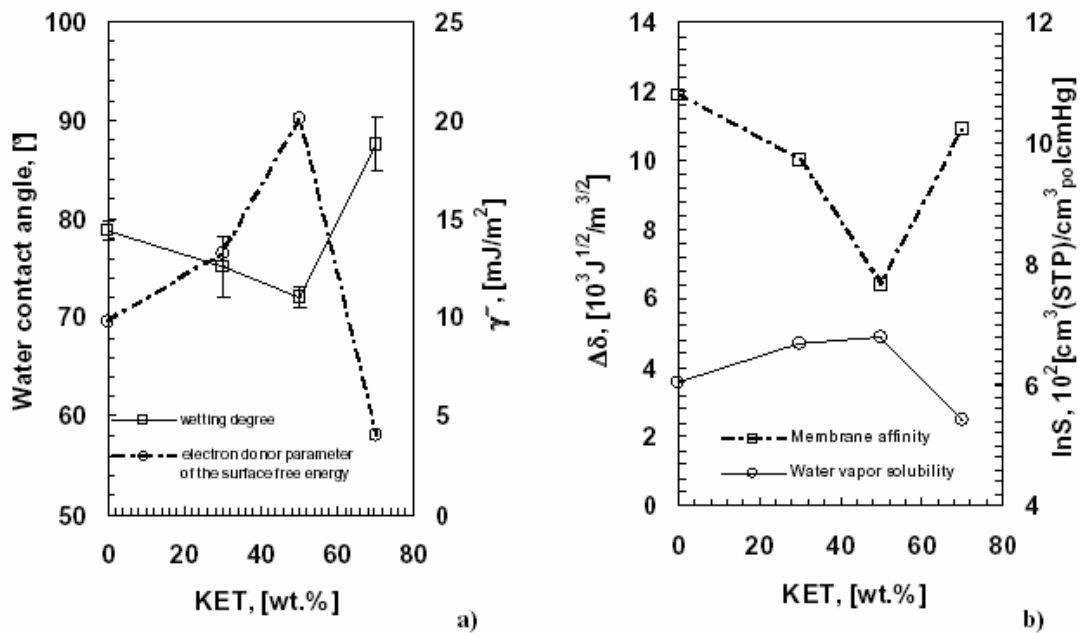
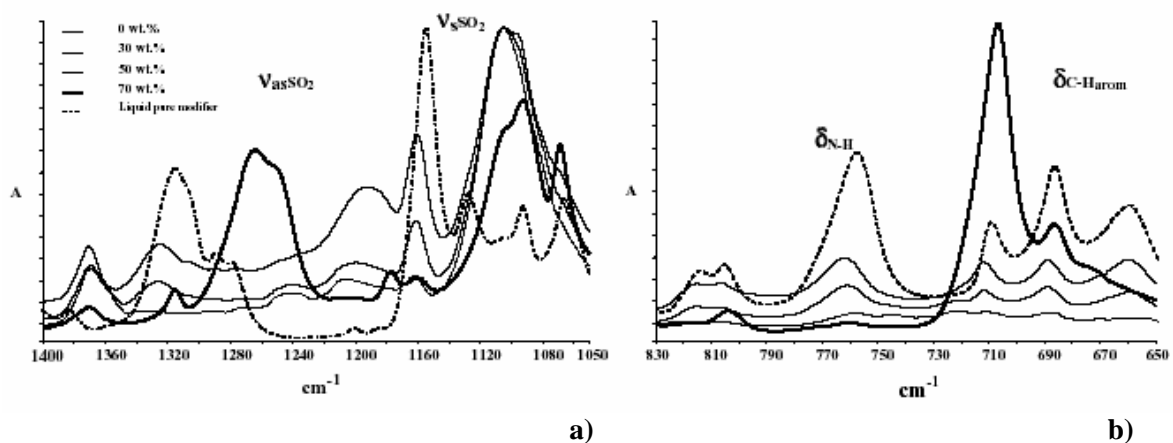


Figure 3 Membrane surface properties estimated for all membranes: a) liquid water wetting degree and electron donor component  $\gamma^-$  [ $\text{mJ}/\text{m}^2$ ] of the overall surface free energy  $\gamma$  [ $\text{mJ}/\text{m}^2$ ] vs KET content into the polymer matrix; b) membrane affinity ( $\Delta\delta$ ), expressed as difference of the membrane-water solubility parameters, and water sorption ( $\ln S$ ) as a function of the KET content.

At higher concentration their accessibility on the membrane surface was drastically reduced. A further increase in modifier content seemed to cancel this positive effect, producing a lowering of  $\Delta\delta$  due to the reduced favourable intermolecular interactions (Figure 3b). These experimental achievements suggest the accessibility of polar moieties as key factor for interpreting the changes in the water sorption into the modified Pebax membranes.



**Fig.2** ATR spectra collected by UATR crystal Diamond/ZnSe: vibrational modes estimated for pure polymer, pure modifier and membranes charged by KET (30-70 wt.%) from 650 to 4000  $\text{cm}^{-1}$  at Res. 4 $\text{cm}^{-1}$ .

ATR analysis yielded important indication about the possible mechanisms which can affect the availability and accessibility of hydrogen donor and acceptor groups. The chemical group accessibility and availability can be attributed to both the changes in polymer packing and to

direct intermolecular interactions involving modifier molecules, respectively. By comparing the spectra of the Pebax/KET membranes with those of the pure polymer membrane and the pure modifier, significant changes in intensity band and vibrational frequency were appreciated as well as the disappearance of specific bands was observed at the highest content in KET (Figure 4). Concerning the stretching of the SO<sub>2</sub> moiety, significant changes in the frequency values were appreciated as the KET content was equal to 70 wt.%. The significant changes observed in the vibrational modes involving the  $\nu_s$ -SO<sub>2</sub>-NR<sub>2</sub> and  $\nu$ -N-H of the sulphonamide linkage indicated that the modifier structures were blocked. This suggests that the sulfonamide linkage is involved in intermolecular interactions, where the amine and oxygen groups of the modifier are linked with another modifier and/or with the polar moieties of the polymer chains (Figures 4a, 4b). Theoretical analysis performed on WP7 have indicated that the key indications highlighted the geometries involving two linked modifiers, establishing the intermolecular interaction N-H $\cdots$ O-S-O, underlying the polymer influence on this interaction.

#### **Publications submitted so far:**

1. M. Macchione, J. C. Jansen, E. Tocci, E. Drioli, Influence of residual solvent on the gas transport properties of dense Hyflon® AD 60X gas separation membranes, *Desalination* 200 (2006) 49-51
2. J. C. Jansen, M. Macchione, E. Drioli "On the unusual solvent retention and the effect on the gas transport in perfluorinated Hyflon AD® membranes" *Journal of Membrane Science* 287 (2007) 132–137
3. M. Macchione, Influence of residual solvent on the thermal, mechanical and transport properties of dense Hyflon AD® gas separation membranes, NYM8 Network Young Membrains, Rende (Italy), 21-23/09/2006
4. M. Macchione J. Jansen, G. De Luca, E. Tocci, M. Longeri, E. Drioli, Experimental analysis and simulation of the gas transport in dense Hyflon\_ AD60X membranes: Influence of residual solvent, *Polymer* 48 (2007) 2619-2635
5. M. Macchione, G. De Luca, E. Drioli, J.C. Jansen Photochromic probes for the analysis of the size distribution of local free volume in amorphous glassy perfluoropolymers of Hyflon AD, 2007 Prague meetings on macromolecules, 47th Microsymposium "Advanced Polymer Materials for Photonics and Electronics" Prague, Czech Republic, 15-19/07/2007
6. PhD Thesis: M. Macchione, Dense Hyflon ® AD membranes for gas separation: influence of the solvent and determination of local free volume. University of Calabria, Italy, 2008
7. A patent application, based on the work on perfluorinated polymers is in progress.
8. A. Gugliuzza, E. Drioli, 'Evaluation of the CO<sub>2</sub> permeation through functional assembled monolayers: relationships between structure and transport', *Polymer*, 46 (23), (2005), 9994-10003
9. A. Gugliuzza, E. Drioli, New self-assembled block co-polyamide membranes: key factors in the control of the transport, oral presentation at ICOM (International Conference on Membrane and membrane processes) meeting, Seoul, Korea.
10. A. Gugliuzza, G. De Luca, E. Tocci, L. De Lorenzo, E. Drioli, "Experimental and theoretical evaluation of the membrane affinity to water: role of modifiers in the control of the matrix performance" *Desalination* 2006, 200: 256-258

#### **Prospect for further use:**

Hyflon AD polymers have proved to be of particular interest for the use in membranes for gas and/or vapour separations. Improved understanding of the transport phenomena in such materials, through the present project, will be valuable for the future development of new membrane materials. One of the findings of the project has given major new insight in the factors which influence the transport properties of perfluorinated polymers and forms now the basis for a patent application (still confidential).

## Task 2.5 UNIBO

### a) Determination of an optimal protocol to obtain Hyflon Ion dispersions with desired water transport behaviour

Experimental study of Hyflon<sup>®</sup> Ion polymers in the presence of water vapour has been carried on to assess guidelines for the preparation of dispersions with satisfactory water sorption capacity. These polymers fall under the category of perfluorosulfonic acid ionomers (PFSI) and they are characterized by a fluorinated, hydrophobic backbone and hydrophilic terminal groups (Figure 1a) so that during hydration water forms interconnected domains (Figure 1b). Such membranes are currently used in fuel cells (FC) as electrolytes. It is well known that FC performance increases with the membrane proton conductivity, which increases with water content in the membrane.

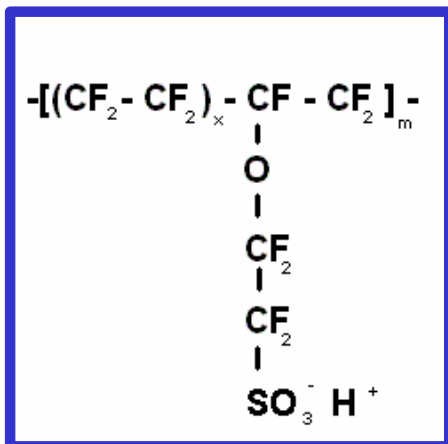


**Figure 1a:** Chemical formula of the monomeric unit of Hyflon<sup>®</sup> Ion H

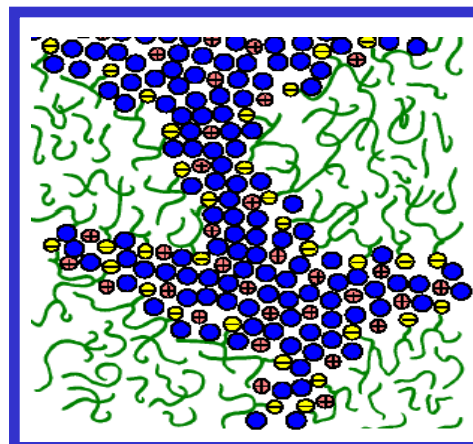


**Figure 1b:** Schematic of the microstructure of a PFSI membrane during hydration

Before the project started, UNIBO, in collaboration with Solvay Solexis, had carried on a complete characterization of extruded films of Hyflon<sup>®</sup> Ion for their launch on the market. During Multimat Design, the attention was moved to films that can be obtained by casting of dispersions: this formulation is particularly useful when thin thicknesses of the films or good adhesion to a substrate are needed. Some formulations were analyzed and, finally, a hydroalcoholic solution without high boiling solvents was chosen, with a specific thermal treatment: such formulation provides the same water vapour solubility and diffusivity as the extruded samples. (Figure 2a and 2b) On the contrary, the formulations containing high boiling solvents such as Dimethylacetamide (DMA) yield a low water uptake.(Figure 2a)

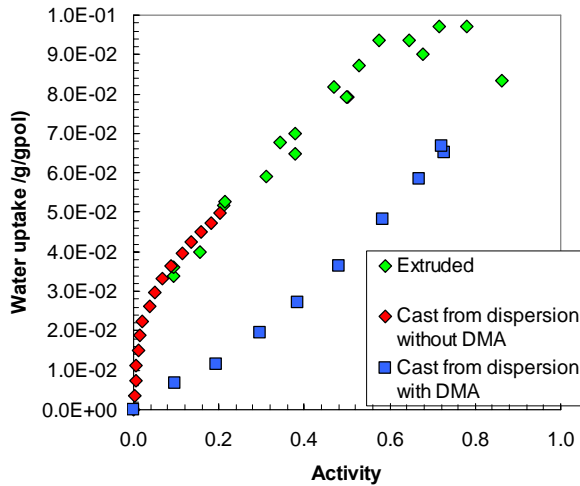


**Figure 2a:** Water uptake in different samples of Hyflon<sup>®</sup> Ion H: *i*) extruded, *ii*) cast from hydroalcoholic dispersion and *iii*) cast from a dispersion containing shigh boiling solvent (DMA).

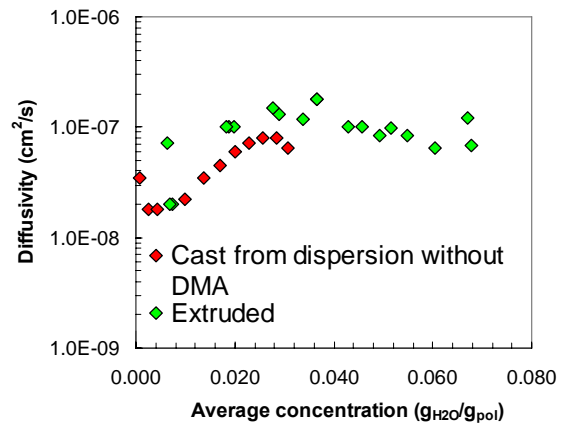


**Figure 2b:** Water diffusivity in different samples of Hyflon<sup>®</sup> Ion H: *i*) extruded, *ii*) cast from hydroalcoholic dispersion.

**b) Experimental support to task 3.2 on mixed matrix membranes modelling (Teflon<sup>®</sup> AF2400 and FS)**

Experimental support was provided to the modelling activity on *mixed matrix membrane* materials performed in Task 3.2, by collecting sorption and transport data of n-C<sub>4</sub> and n-C<sub>5</sub> on composite materials of a fluorinated high free volume glassy polymer (Teflon<sup>®</sup> AF2400) and a hydrophobic nanoscopic impermeable filler (Fumed Silica FS) (see Figure 3). Surprisingly, such composite materials show higher permeability than the pure polymer matrices, due to the fact that the filler modifies the microscopic arrangement of polymeric chains in a way that increases the free volume available for gas penetration; this effect overcomes the fact that FS particles depress permeation by creating a physical barrier to gas molecules.

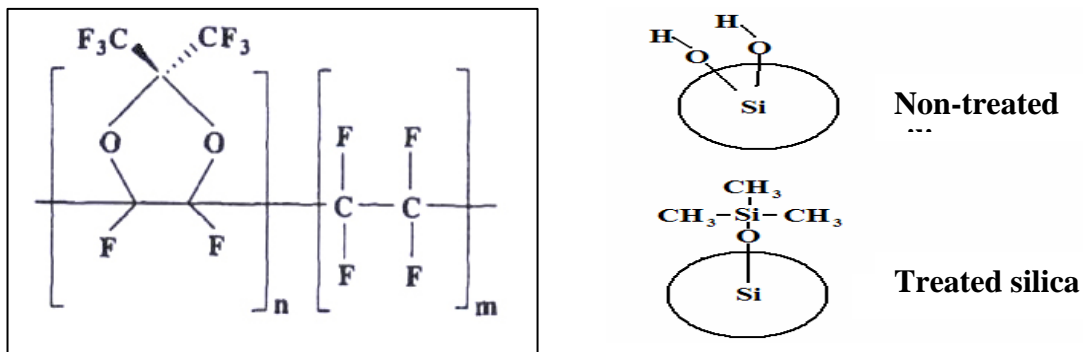


**Figure 3:** Chemical formulas of Teflon AF2400 and hydrophobic fumed silica (FS)

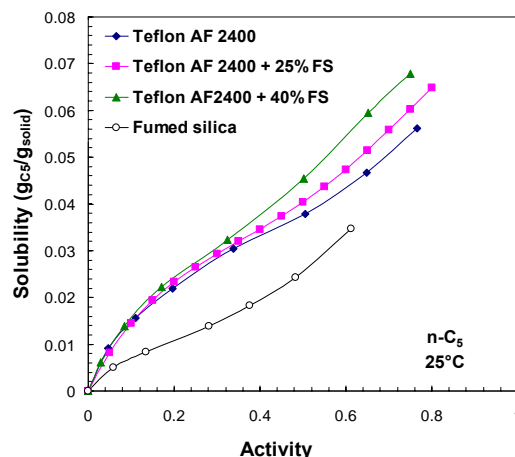
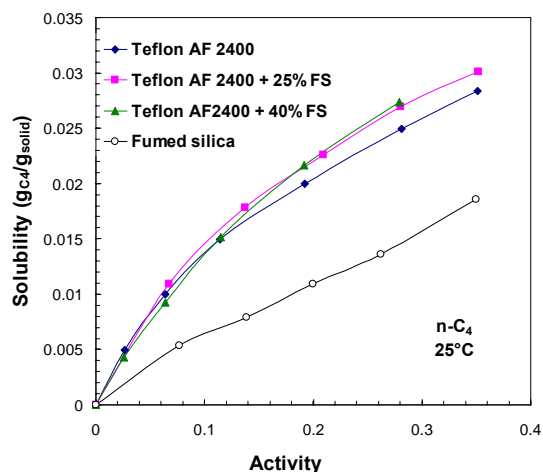


**Figure 4a:** Solubility of n-C<sub>4</sub> in pure AF2400, AF2400+25%FS and AF2400+40%FS, and adsorption onto pure fumed silica at 25°C, in grams of penetrant per gram of total solid

**Figure 4b:** Solubility of n-C<sub>5</sub> in pure AF2400, AF2400+25%FS and AF2400+40%FS, and adsorption onto pure fumed silica at 25°C, in grams of penetrant per gram of total solid

Solubility (Figure 4) and diffusivity (Figure 5) isotherms of n-C<sub>4</sub> and n-C<sub>5</sub> in 3 materials containing various amounts of FS were obtained. The results shows that both the diffusivity and the solubility increase with FS content due to increased free volume. On the other hand, the swelling coefficient remains essentially constant with FS loading: this is due to the fact that filler varies only the chain packing and not the mobility of polymeric chains. This behaviour was represented satisfactorily with the model presented in Task 3.2.

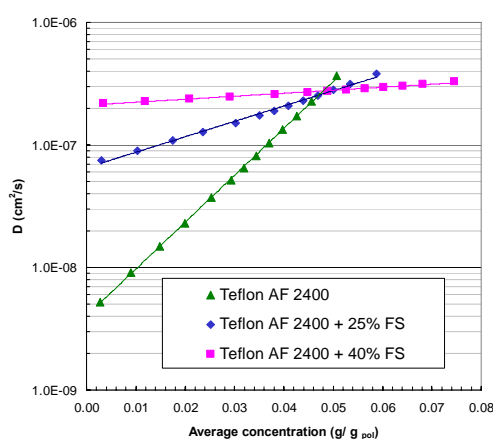
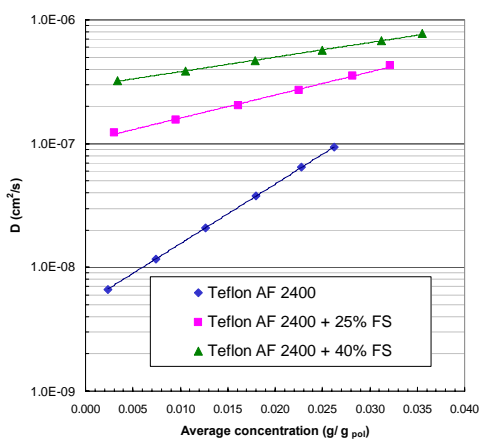


**Figure 4a:** Diffusivity of n-C<sub>4</sub> in AF2400-based mixed matrices at 25°C, versus average penetrant concentration in the step.

**Figure 4b:** Diffusivity of n-C<sub>5</sub> in AF2400-based mixed matrices at 25°C, versus average penetrant concentration in the step.

### c) Vapor sorption in modified polynorbornene membranes synthesized by TIPS

A characterization of modified polynorbornene membranes synthesized by TIPS was carried on in the presence of pentane and hexane vapours. The choice of this polymer was motivated by the fact that it showed, during inverse gas chromatography measurements at TIPS, very high infinite dilution gas solubility and therefore seemed a promising candidate for gas separation applications. Our results served to implement the characterization carried on at

TIPs and in particular to broaden the range of pressure inspected in solubility measurements, to determine the diffusivity and the permeability of the films and to characterize the vapour-induced swelling of the films, that is an important indicator of the plasticization occurring in the polymer membrane. Plasticization has to be avoided in order to maintain a high selectivity. Our results show that low pressure solubility has the same value as the one measured at TIPs, moreover, the permeability of the more condensable and larger hexane is higher than that of pentane, which is a typical feature of high free volume glassy polymers such as PTMSP.

#### **Publications submitted so far:**

- L. Basile, M.C. Ferrari, M.G. De Angelis, T.C. Merkel, G.C. Sarti "Sorption and Diffusion of Organic Vapors in Mixed Matrices Based on Teflon AF2400 and Fumed Silica" AIChE 2007 Annual Meeting November 4-9, 2007, Salt Lake City, UT.
- M. C. Ferrari, J. Catalano, M. Giacinti Baschetti, M. G. De Angelis, and G. C. Sarti "Water transport in a short side chain PFSI membrane: Differences between cast and extruded membranes subject to different thermal treatments" PMSE Preprints. 232TH NATIONAL ACS MEETING. San Francisco, CA. September 10-14, 2006. (vol. 95).
- M. C. Ferrari, J. Catalano, M. Giacinti Baschetti, M. G. De Angelis, G. C. Sarti. (2006). Water Transport in a Short Side Chain Pfsi Membrane: Differences between Cast and Extruded Membranes Subject to Different Thermal Treatments. 2006 AIChE Annual Meeting and Fall Showcase Conference Proceedings 12-17 November 2006, San Francisco, CA.
- Y. Yamamoto, M. C. Ferrari, M. Giacinti Baschetti, M.G. De Angelis, G.C. Sarti "A quartz crystal microbalance study of water vapor sorption in a short side-chain PFSI membrane", EUROMEMBRANE 2006, Giardini Naxos, 24-28 September 2006.

#### **Prospect for further use:**

The experimental data on Hyflon Ion will be used as basic transport parameters by final users, the data on PNB will be used by the modeller and the designer of gas separation membranes.

#### **WP3: "Design of High Performance Polymer Membranes for Selective Gas Separations"**

The objective of WP3 was to propose a CAMD methodology for the rational design of novel membranes made of functional and structural polymers or composites showing superior performance, by controlling their nano-structure. For realising this goal a multi-scale CAMD approach combining atomistic, Finite elements (FE), Quantitative Structure Property/Activity QS(P/A)R and Thermodynamic simulation tools has been developed for supporting experimental development of potentially attractive polymer-based membrane materials targeting the air separation and natural gas purification applications. The suggested materials should in particular show a much improved trade-off between permeabilities and selectivities.

For reaching these goals considerable effort has been spent on two axes:

- Methodological development and application of multi-scale simulation techniques including their specific development and validation. This work includes the model development as well as methodological improvements in the way the tools are used :
  - Atomistic Simulation of gas transport through Membranes
  - QSPR/QSAR based prediction of thermodynamic and transport properties
  - FE modelling of mixed matrix membranes and their optimisation
  - Thermodynamic modelling through Lattice-fluid model
  - Atomistic modelling of polymer ageing

- Application of the above mentioned simulation techniques for assessing real life problems like optimal design of polymer Repeat Unit (RU) for obtaining high performance membranes to be used in:
  - Glassy polymer membranes for improved air separation
  - Mixed matrix membranes for air separation
  - Mixed membrane design for HC and natural gas purification applications
  - Design rules for avoiding polymer ageing

It is to note that from the beginning one of the difficulties has been to effectively combine these simulation methods and be able to pass information from a more detailed method to a coarser one. In the following we briefly resume the important steps of each method and give information on how the information obtained by one is used in the other.

Atomistic Simulation of gas transport through Membranes: The estimation of the diffusion coefficient  $D$  and of the solubility coefficient  $S$  of small permeate molecules in a polymeric membrane is strongly dependent on the quality of the amorphous cell used in the calculation. This is particularly true in the case of stiff chain polymers containing aromatic moieties. In WP3 more than 70 Repeat units (RU) and more than 300 independent atomistic bulk models were generated (at least 3 cells for a RU). The cubic basic volume element first has been filled with segments of a growing chain under periodic boundary conditions following a combination of the Theodorou-Suter chain-generation approach and the Meirovitch's scanning method for reproducing the natural distribution of conformation angles. We improved the AC construction methodology by inserting “solvent” molecules in the initial phase of amorphous cell construction in order to avoid ring ring-catenation. Multistage equilibration procedures after sequential removal of “solvent” molecules followed by energy minimisation and MD simulations have been used in order to reproduce realistic models of the polymer membranes. We have used the “FFV distribution” as a descriptor of the “goodness” of each packing at an intermediary stage of construction. After the elimination of the non-realistic boxes we have finally generated 3-4 realistic amorphous cells for each of the polymers. During the final amorphous cell generation the conformation and non-bonded pair interaction terms in the force field (torsion, non-bonded and coulomb interactions) have been first appropriately scaled down by 1:1000 followed by 1000 steps of conjugate gradient minimization and 1ps of

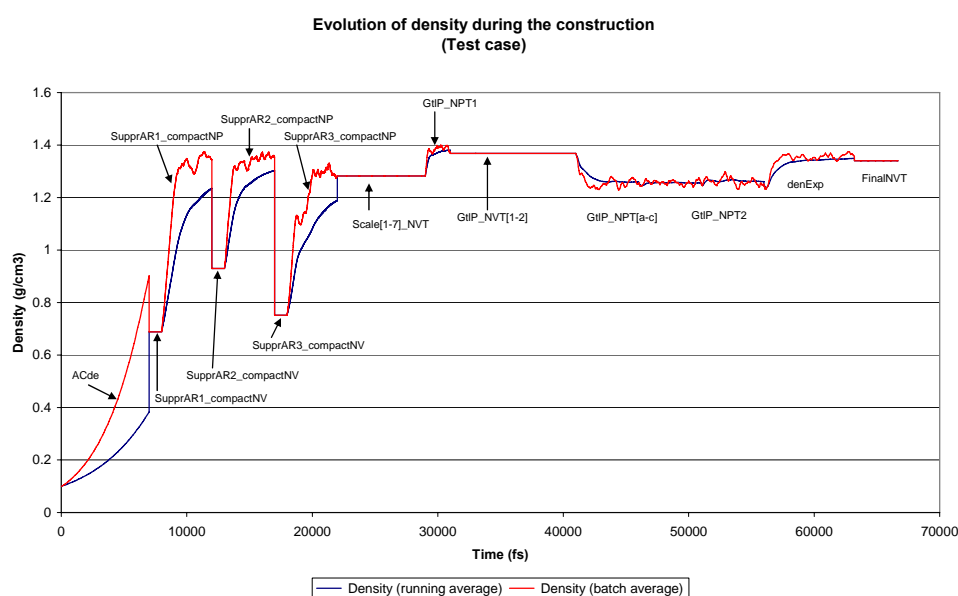


Figure 3.1 Density profile evolution in the process of generation of realistic membrane models

NPT dynamics and then the interactions were scaled up to original values in 6 steps (torsions in three steps 1:100, 1:10 and 1:1 with intermediary minimisation and NPT 1ps relaxation followed by “non-bonded and coulomb” in three steps 1:100, 1:10 and 1:1 with intermediary minimisation and NPT 1ps). Finally a series of seven MD 5ps compression runs [(NPT,1GPa, 300K) (NVT, 600K) (NVT, 300K) (NPT, 0.1GPa, 300K) (NPT, 0.01GPa, 300K) (NPT, 0.001GPa, 300K) (NPT, 0.0001GPa, 300K, 30ps)] followed by 300ps NVT (300K) have been performed for each amorphous cell to match the experimental density as reported in figure 3.1

The transition state theory (TST) as implemented in InsightII (400P+), has been used to study the thermodynamics and transport of the small gas molecules, oxygen, nitrogen and carbon dioxide, respectively, in selected polymer packings. Diffusion coefficients (D) and gas solubility (S) in the matrix have been estimated. The calculation has been carried out in two steps. In the first step, the solubility (S) of the respective gas is evaluated. A 3D orthogonal lattice grid with a constant spacing of 0.3 Å has been used to estimate solute distribution function in the matrix by calculating the Helmholtz free energy between the gas molecule inserted at each grid point and all the atoms of the polymer matrix that are subject to elastic fluctuations. These data are used to identify minimum energetic sites and determine transition probabilities from site to site together with the residence times in each site. It is to notice that the memory limitation (maximum number of sites=600) of the gsnet-code has been removed allowing to use the same the grid spacing for all generated cells. In the calculation of D carried out with gsdif the two important parameters are:

- the simulation time :  $\log(t_{\max})$  : sufficiently long simulations to be significative.
- the number of trajectories calculated : the more trajectories, the more accurate the statistic analysis will be.

For some permeate molecule  $\log(t_{\max})=-5$  is sufficient (Helium) and for other molecules we have to set  $\log(t_{\max})=-2.5$  (CO<sub>2</sub>). As this is a logarithmic scale there is a factor 10 in simulation time (and CPU time) when  $\log(t_{\max})$  changes from -4 to -3.

In general one can say that the simulation time is sufficient if grad (MSD(gaz)) tends to 1. In Figure 3.2 it is shown that O<sub>2</sub>, N<sub>2</sub> and He reach the equilibrium but CH<sub>4</sub> and CO<sub>2</sub> do not reach it. The total simulation time is  $10^{-4.5}$  s

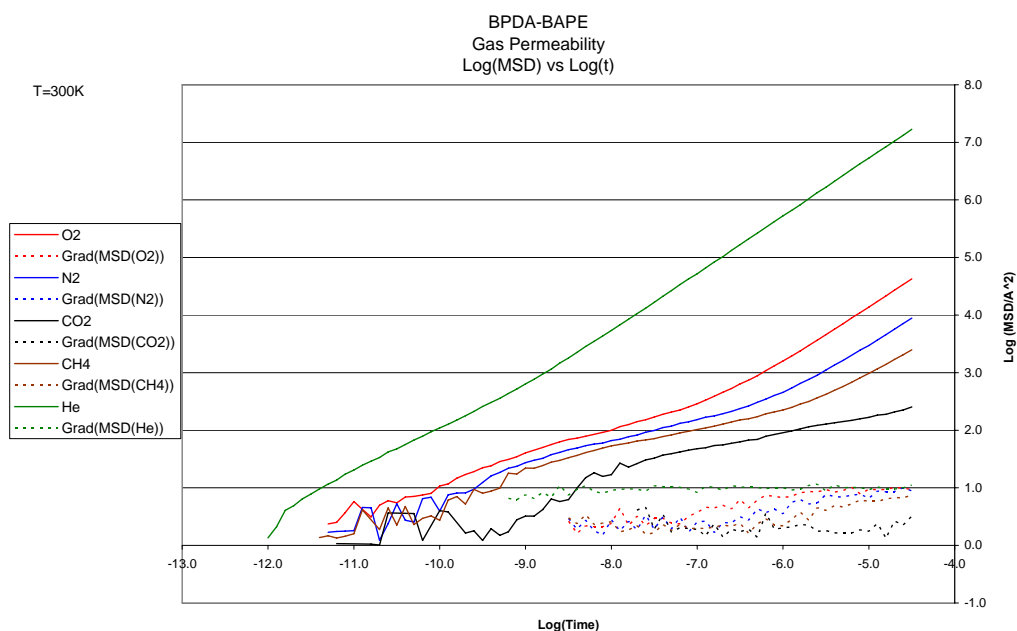


Figure 3.2 Variation of MSD with time (logarithmic scale) for several gases in BPDA-BAPE

*QSPR/QSAR based prediction of thermodynamic and transport properties:* The results of calculations that have been performed in step 1 (atomistic simulation of membrane properties) have been used in the QSAR/QSPR approach developed in WP3 for construct a quantitative correlation between structural characteristics of atomistic-simulated membrane and RU models (3D-cells, RU) and TST-predicted transport properties of small gas molecules (O<sub>2</sub>, N<sub>2</sub>, CO<sub>2</sub>, CH<sub>4</sub> and He) through these membranes. The first step in the QSAR model development consists in definition of meaningful descriptors followed by their calculation for all the 3D-cells and the RU of the dataset. Since experimental descriptors can be time-consuming to determine and require that a membrane be available for experimentation, we have selected to use only theoretical descriptors, which can be directly calculated using the molecular representation of a membrane at different levels of representation. For instance, the lowest level of structural information would contain only the composition, such as number and type of atoms. At the next level, the basic connectivity information would allow fragment count using different descriptors. A fragment is a specific functional group and these fragment count descriptors have found wide use in group contribution methods. Continuing on, the three-dimensional structure of a RU can be used for descriptor calculation. Important developed descriptors concern the characterization of the FFV (Fractional Free Volume) and FFFD (Fractional Free Volume Distribution) of the generated cells during the first two years of the project. These numerical descriptors allow varying levels of structural information to be used depending upon the level of information needed. In practice, descriptors are typically correlated with one another to varying degrees. The number of descriptors that are available or that we have developed during the third year of the project is extremely large. This allows a high degree of freedom in creating structure/property relationships, but it also introduces the need to preferentially select the optimal descriptors for establishing useful structure-property relationships. Search through this descriptor space and reduction it down to the most significant descriptors has been carried out as a first step toward constructing a QSAR model. Some simple techniques include eliminating descriptors that are nearly constant for all compounds and discarding one of a pair of descriptors that are highly correlated. The analysis of the correlation matrix for all the calculated descriptors allows identifying groups of highly correlated ones and selection of only less correlated ones. In figure 3.3 the correlation matrix on a selection of descriptors is reported showing several groups of cells colored in red corresponding to highly correlated elements.

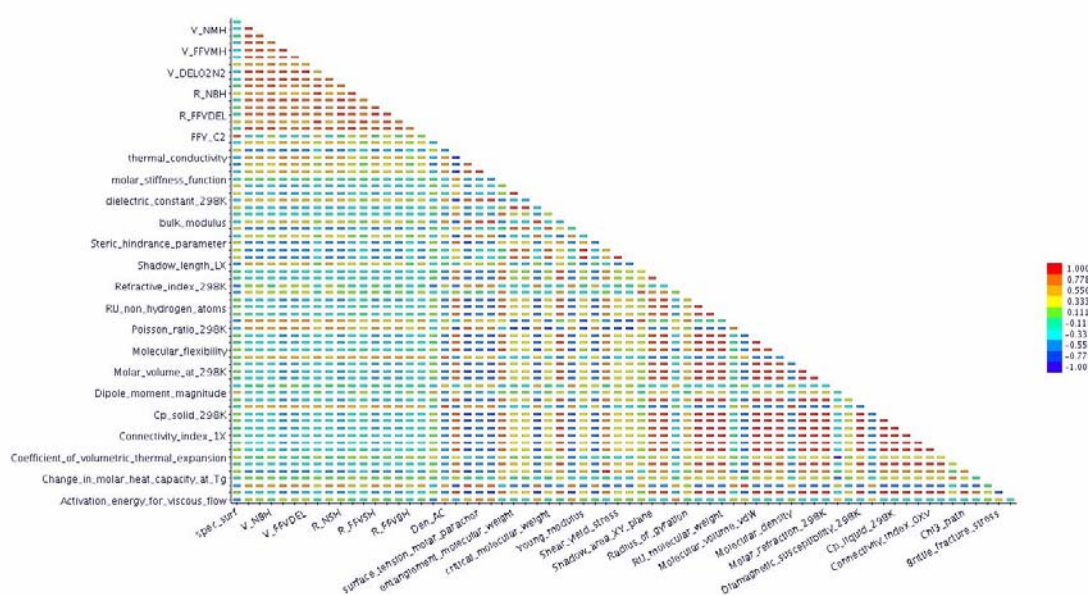


Figure3.3: Correlation matrix for a selected set of descriptors.

More involved techniques use tools such as principal component analysis or cluster analysis to eliminate descriptors while retaining the original information of the full descriptor set have been used during the QSAR-RU study. Performing this initial pruning of the descriptor pool simplifies the following process of selection and model building. Typically the process of descriptor selection and model building has been conducted simultaneously.

After the selection of final descriptors we used a regression method to create the structure-property relationship. For all work shown reported in the project, the Genetic Function Approximation (GFA) has been used to select the most important descriptors and create the optimal linear relationship. The first step of the GFA algorithm is to randomly generate an initial population of equations. , the S(O2) values of the dataset Cells are predicted using the QSAR model constructed from the training set. Small differences (residuals) between corresponding observed and predicted S values of the test set compounds indicate high predictivity of the individual QSAR model. In figure 3.4 the variable usage in establishing the correlation based on GFA is reported.

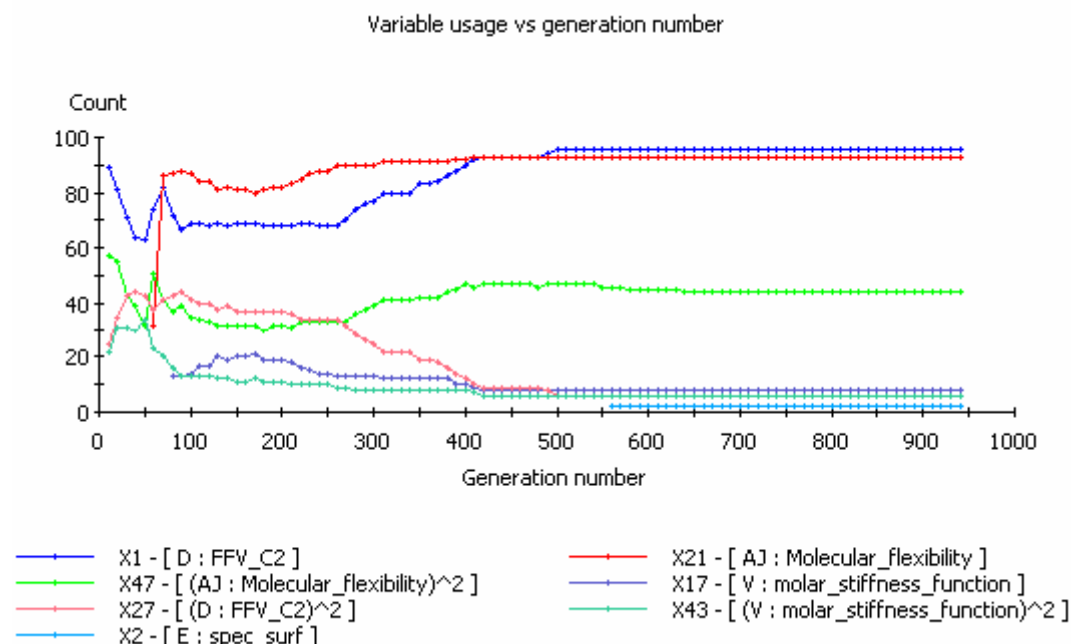


Figure 3.4: Variable usage in generating the QSARmodels for the Solubility.

As it appears clear from the figure the most used descriptors are the FFV-C2 which is the fractional free volume of the membrane as calculated with MS (Accelrys) software and the Molecular flexibility which is related to the RU structure. Several GFA equations have been generated. In the following only two of them are reported.

Equation 1 :

$$Y = 16.262482438 * X1 - 0.215447626 * X21 + 1.873330021$$

X1 : FFV\_C2

X21 : Molecular\_flexibility (RU)

Equation 5 :

$$Y = 17.314854798 * X1 - 0.268050978 * X21 + 0.025494602 * X22 + 1.590652525$$

X1 : FFV\_C2

X21: Molecular\_flexibility (RU)

X22 : Chi3\_path

In figure 3.5 the Solubility values for the TST-calculated (blue) are compared with QSAR-eq1-predicted (red) and QSAR-eq5-predicted (green)

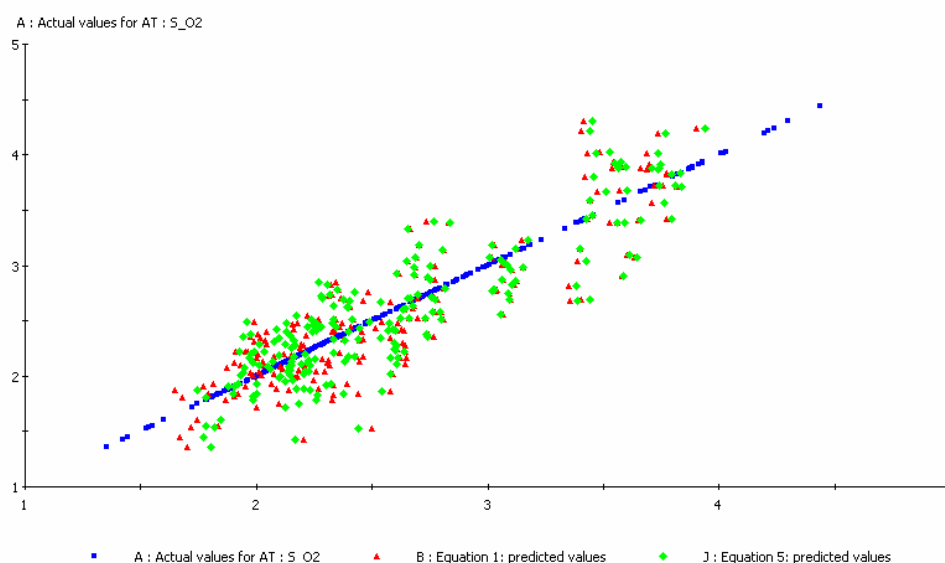


Figure 3.5: Comparison of TS-Calculated with QSAR-predicted S(O<sub>2</sub>) Values.

The same approach has been used for finding a correlation for the predicting of D(O<sub>2</sub>). We have found several QSAR models. However contrary to S(O<sub>2</sub>) predictions where the equations are linear combinations of descriptors for the D(O<sub>2</sub>) models the descriptors appear as squares or product of two of them. This implies that the generated correlations for D(O<sub>2</sub>) should be used more for interpolation than for extrapolation purposes. For design purposes it is desirable to find correlations between molecular features of the RU (structures and properties of the RU) and the gas transport properties of the membranes. For this we have adopted a multilevel QSAR. After defining the correlations between S(O<sub>2</sub>) and D(O<sub>2</sub>) and the descriptors of the cells and RUs, we looked for correlations between the Cells descriptors that were used in these correlations and the descriptors of the RU alone. In Figure 3.6 is reported the GFA generated correlation describing the FFV as a function of descriptors of the RU.

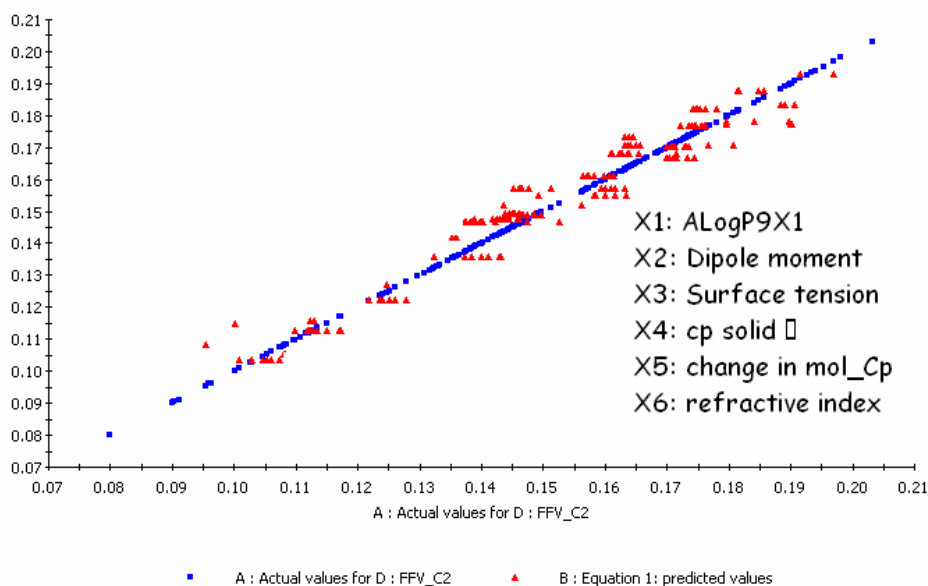


Figure 3.6: Comparison of Calculated with QSAR-predicted FFV Values (equation 1)

$$\text{FFV\_C2} = -0.025660562 * X1 + 0.003183677 * X2 - 0.000050232 * X3 + 0.000000173 * X4 + 0.000001748 * X5 - 0.095741942 * X6 + 0.63288623$$

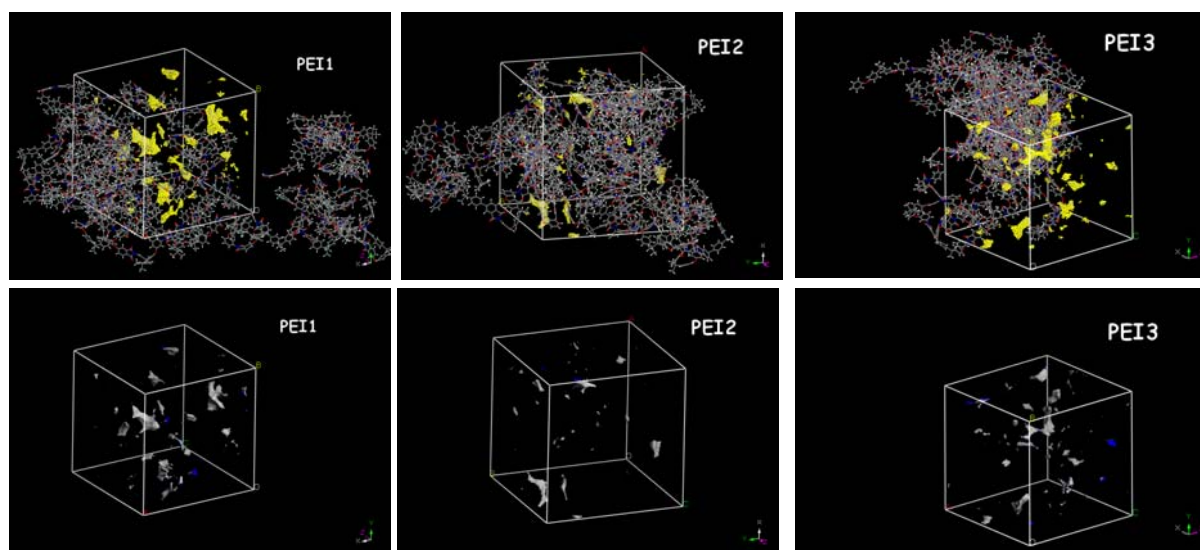


Figure 3.7: Calculated FFV of PEI membrane packings

In order to validate the correlation, newly synthesized membranes PEI1, PEI2 and PEI3 as well as the PIM membrane have been used. The packing models of these membranes have been generated and the FFV analysis of the cells has been carried out as reported in Figures 3.7 and 3.8.

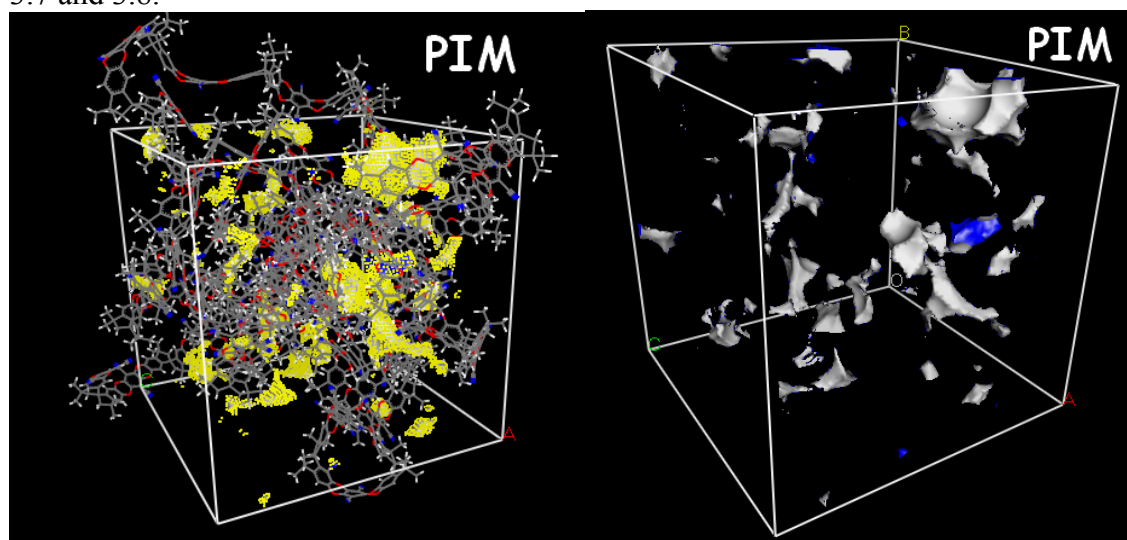


Figure 3.8: Calculated FFV of PIM membrane packing

The numerical values of Volume calculations with the MS software are reported in Table 3.1.

Table3.1: Calculated volumes and surfaces of new membrane packings

<b>Pim</b>	<b>PEI1</b>	<b>PEI2</b>	<b>PEI3</b>
<i>Connolly Surface</i>	<i>Connolly Surface</i>	<i>Connolly Surface</i>	<i>Connolly Surface</i>
Occ_Vol: 30735.04 Å <sup>3</sup>	Occ_Vol: 37584.15 Å <sup>3</sup>	Occ_Vol: 36446.39 Å <sup>3</sup>	Occ_Vol: 36618.24 Å <sup>3</sup>
Free_Vol: 23005.17 Å <sup>3</sup>	Free_Vol: 16531.69 Å <sup>3</sup>	Free_Vol: 13678.53 Å <sup>3</sup>	Free_Vol: 17363.41 Å <sup>3</sup>
Surf_Area: 25362.28 Å <sup>2</sup>	Surf_Area: 25396.86 Å <sup>2</sup>	Surf_Area: 23446.32 Å <sup>2</sup>	Surf_Area: 26119.65 Å <sup>2</sup>
<i>Solvent Surface @1.4</i>	<i>Solvent Surface @1.4</i>	<i>Solvent Surface @1.4</i>	<i>Solvent Surface @1.4</i>
Occ_Vol: 52275.69 Å <sup>3</sup>	Occ_Vol: 53859.46 Å <sup>3</sup>	Occ_Vol: 50053.50 Å <sup>3</sup>	Occ_Vol: 53791.89 Å <sup>3</sup>
Free_Vol: 1464.52 Å <sup>3</sup>	Free_Vol: 256.39 Å <sup>3</sup>	Free_Vol: 71.42 Å <sup>3</sup>	Free_Vol: 189.77 Å <sup>3</sup>
Surf_Area: 3176.23 Å <sup>2</sup>	Surf_Area: 752.45 Å <sup>2</sup>	Surf_Area: 256.22 Å <sup>2</sup>	Surf_Area: 623.61 Å <sup>2</sup>
<i>Acc_Solv_Surf @1.4</i>	<i>Acc_Solv_Surf @1.4</i>	<i>Acc_Solv_Surf @1.4</i>	<i>Acc_Solv_Surf @1.4</i>
Occ_Vol: 52942.67 Å <sup>3</sup>	Occ_Vol: 54028.17 Å <sup>3</sup>	Occ_Vol: 50083.73 Å <sup>3</sup>	Occ_Vol: 53938.52 Å <sup>3</sup>
Free_Vol: 797.54 Å <sup>3</sup>	Free_Vol: 87.67 Å <sup>3</sup>	Free_Vol: 41.19 Å <sup>3</sup>	Free_Vol: 43.13 Å <sup>3</sup>
Surf_Area: 1585.11 Å <sup>2</sup>	Surf_Area: 259.39 Å <sup>2</sup>	Surf_Area: 132.93 Å <sup>2</sup>	Surf_Area: 150.68 Å <sup>2</sup>

In Table 3.2 are reported the QSAR predicted (equation 1) together with calculated values of the FFV. The QSAR predictions agree well with the calculated values of the FFV. It is to notice that the calculated value of PIM is out of the range of the values of the cell dataset that have been used for generating the correlation. In this way we have validated the correlation not only for interpolation use but also in extrapolation which shows the strength of the obtained correlation.

Table 3.2: Comparison of calculated to QSAR-predicted FFV.

<b>Name</b>	<b>ALogP98 (X1)</b>	<b>Dipole moment (X2)</b>	<b>Surface tension (X3)</b>	<b>cp solid (X4)</b>	<b>change in mol_Cp (X5)</b>	<b>refractive index (X6)</b>	<b>Predicted FFV</b>	<b>calculated FFV packing cell</b>
RU_PIM1	5.9720	3.2397	51.5013	530.5018	7.5201	1.6694	0.3276	0.3059
RU_PEI1	14.0564	13.8291	47.8191	1058.4450	119.9395	1.6071	0.1603	0.1635
RU_PEI2	13.7442	5.8595	47.8789	1000.2570	190.3856	1.6379	0.1401	0.1180
RU_PEI3	10.7534	9.6286	48.8541	860.2681	173.6490	1.6412	0.2285	0.1954

Several correlations have been found also for describing the Specific\_Surface in term of RU descriptors (equations 1 to 3) but the QSAR-predictions could be used only for interpolations and are very sensible to RU descriptors. New RU descriptors are needed for developing highly predictive SS-QSAR models.

**Accelrys:** Calculating the distribution of the free volume in the polymer is a vital descriptor for the prediction of permeability using bulk atomistic models. A method has been implemented in Materials Studio which allows overall free volume to be calculated. This was extended to include the ability to segregate the free volume data and hence access descriptors

such as the volume distribution, fitted radius size distribution, and segregate separation. For single system, charts can be generated of the different analysis above. A scripting interface has been provided which allows the bulk prediction for a range of structures and provides a framework for custom analysis. With the use of scripting, this allows the integration of atomistic free volume data into standard QSAR.

In an additional activity by partner **MatSim** a coupled-form finite element approach was introduced and implemented to estimate the permeability performance of mixed matrix nanotube/polymer membranes. It appeared that the universal approximation of perfectly permeable nanotubes was appropriate for predicting the overall rates of single gas transport through CNT/polymer membranes. Based on direct finite element predictions, we developed a set of simple design equations and demonstrated that mixed matrix CNT/polymer membranes can favorably combine the high-flux performance of nanotubes with the intrinsic selectivity of polymer matrix. (Adv. Mater. **2007**, 19, 2672-2676)

The finite element method was used to analyze the role of filler aspect ratio and volume loading on the effective permeability and selectivity of gas-separation membranes consisting of a polymer matrix filled with molecular sieve particles of platelet shape. On the basis of direct 3D finite element estimates we develop and validate a quick arithmetic procedure for predicting the effective permeability and selectivity of platelet-filled systems. By using this procedure, we have analyzed the trade-off between the permeability and selectivity of mixed matrix membranes composed of Zeolite platelets dispersed in a PDMS matrix. We have demonstrated that by using platelets of aspect ratio 100 and more, one can achieve permselectivity values considerably exceeding the Robeson's upper bound even at already small particle volume fractions of 0.1-0.3 (Figure 1) (J. Membr. Sci. **2008** (submitted)).

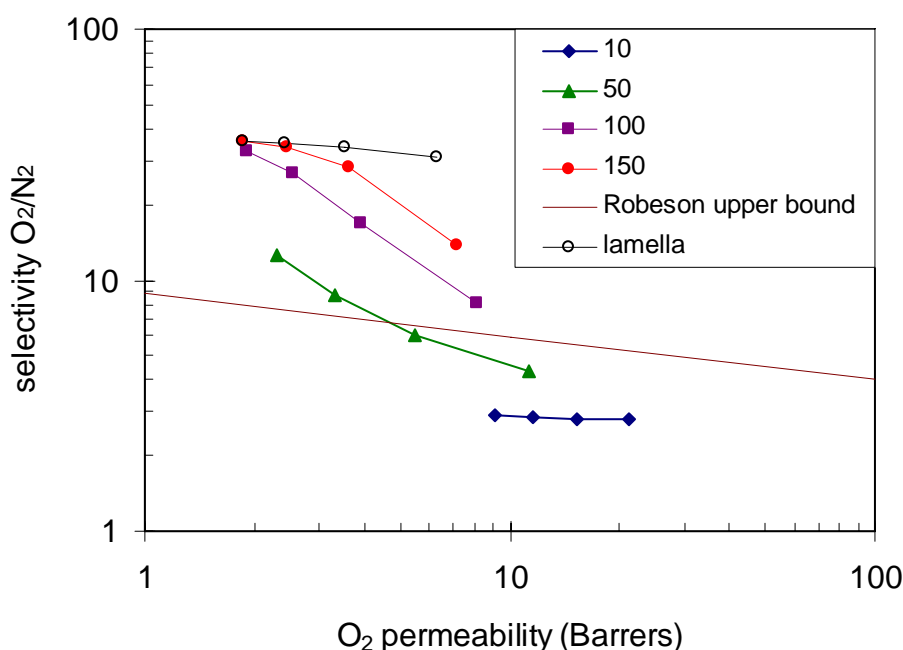


**Figure 1** Predicted zeolite-platelets/PDMS matrix membrane performance. For each symbol kind, the point on the right corresponds to a volume fraction of 0.1, then to the left the volume fraction increases as 0.2, 0.3 and 0.4 (the left point)

### Task 3.2 UNIBO

A macroscopic method has been developed to evaluate the fractional free volume (FFV) variation induced by filler addition in composite systems formed by glassy polymers and impermeable inorganic spherical particles and it has been tested on systems formed by

PTMSP, Teflon AF2400 and Fumed Silica and various penetrants. The FFV variation induced by filler addition is difficult to estimate precisely with traditional methods such as the measurement of composite density due to intrinsically high experimental error, but is a required parameter in order to predict the variation of diffusivity with filler loading: in our method we use the solubility of one test penetrant in the composite materials to evaluate the FFV variation, by means of the NELF model (see Figure 1). The method has been successfully used on literature data of gas permeation in Teflon AF2400/FS and PTMSP/FS composites, based on the experimental solubility data relative to n-butane.

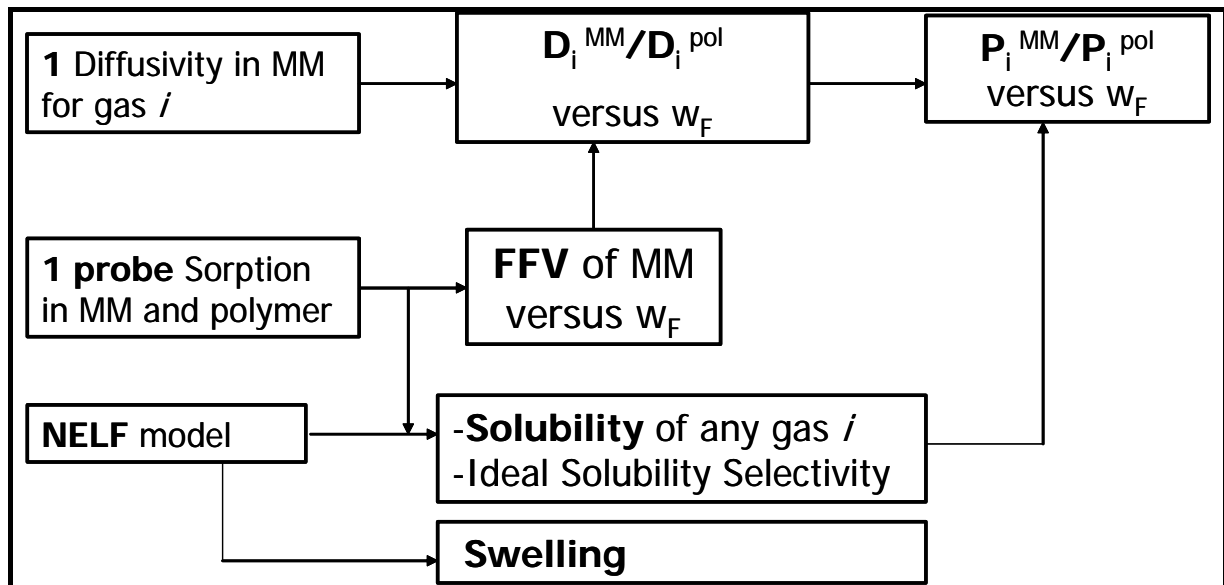


**Figure 1:** Scheme of the method proposed for description of mixed matrices transport behaviour

The modelling is based on the observation that the gas sorption in the composite does not obey an additive rule. We assumed that the reason for such behaviour lies in the fact that the polymeric phase has an higher free volume with respect to the pure polymer state and therefore a higher sorption capacity. With NELF model we can relate solubility variations of one probe gas to density variations of the polymeric phase and, consequently, to FFV variations. The FFV values found in these way can be used to:

- predict the solubility of other gases in the same matrices
- predict the variation of diffusivity of the probe gas and of other gases with one adjustable parameter

Moreover, the NELF model allows to evaluate the swelling induced by the probe penetrant.

For the sake of brevity we exemplify the procedure on literature data obtained by Merkel on composites formed by PTMSP and Teflon AF2400, but we must say the same procedure has been applied successfully to the data collected in Task 2.5 on Teflon AF2400 composites.

In Figure 2 we report the procedure to evaluate the FFV based on the solubility isotherms in the polymeric fraction of the composites: the value of glassy polymer density in the NELF model is varied so to correctly represent the solubility isotherms. The values of density obtained, as well as FFV values, are reported in Table 1.

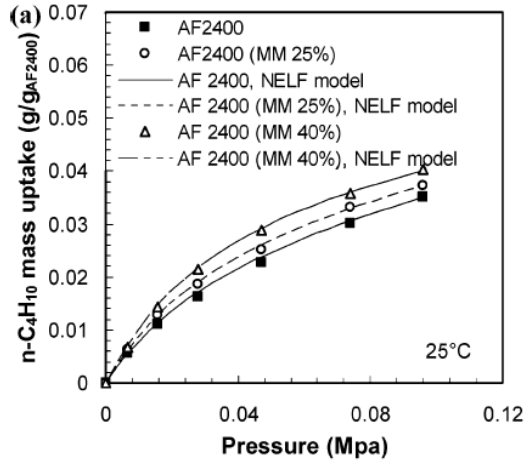


Figure 2a: Solubility of  $n\text{-C}_4\text{H}_{10}$  in Teflon AF 2400 and related mixed matrices at 25 °C and NELF model predictions.

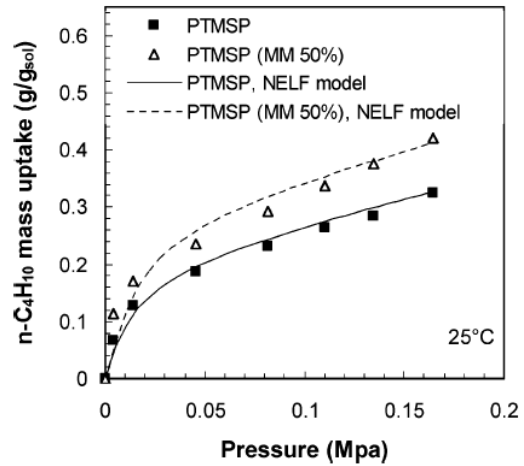


Figure 2b: Solubility of  $n\text{-C}_4\text{H}_{10}$  in PTMSP and related mixed matrices at 25 °C and NELF model predictions.

**Table 1**

Material	$w_F$	$\Phi_F$	$\rho_2^0$ (kg/L) at 25°C	Tortuosity factor $\tau$	FFV	$k_{sw}$ ( $\text{MPa}^{-1}$ )
AF 2400	0.0	0	1.740	1	0.319	0.264
AF 2400/25FS	0.25	0.209	1.714	1.104	0.329	0.195
AF 2400/40FS	0.40	0.345	1.680	1.173	0.343	0.100
PTMSP	0.0	0	0.750	1	0.290	0.90
PTMSP/30FS *	0.30	0.127	0.718	1.064	0.320*	0.90
PTMSP/40FS *	0.40	0.185	0.702	1.093	0.336*	0.90
PTMSP/50FS	0.50	0.254	0.680	1.127	0.356	0.90

The diffusivity in the polymeric phase of the composite, at infinite dilution obeys the following equation:

$$\ln(D_p(0)) \propto -\frac{1}{FFV}$$

And it is related to the composite diffusivity, that is the directly measurable quantity, through the following relationship:

$$D_p(0) = \tau \cdot D_M(0)$$

Where  $\tau = 1 + \frac{\Phi_F}{2}$  is a tortuosity factor given by Maxwell's model for spherical impermeable particles. The results obtained for the diffusivity of various penetrants in mixed matrices of PTMSP and AF 2400 with the values of FFV obtained from the above procedure are shown in figure 3 and they are very well correlated by the above equations, represented by the solid lines: this result states that the FFV values obtained are quite reliable and can be used to predict transport behavior. This is a very valuable tool for the modelling of these peculiar composite matrices, whose behaviour cannot be predicted by conventional model for composites that would predict a lower permeability in the composite than in the pure polymer.

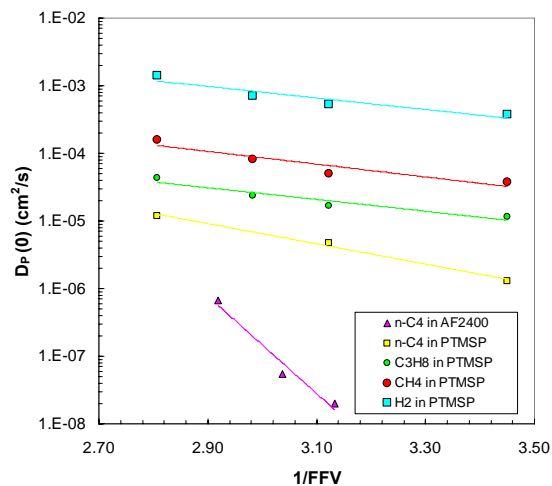


**Figure 3:** Values of  $D_p(0)$  versus  $1/FFV$  for gas diffusivity in the polymer phase of mixed matrices of PTMSP and FS and AF2400 and FS at 25 °C.

**Publications submitted so far:**

M.G. De Angelis, G.C. Sarti “Solubility and diffusivity of gases in mixed matrix membranes containing hydrophobic fumed silica: correlations and predictions based on the NELF model”, *Ind. Eng. Chem. Res.* 10.1021/ie0714910

**Prospect for further use:**

During the project the model developed has been validated sufficiently on literature and self-obtained experimental data and will now be adopted routinely as a tool for the modelling and design of composite materials based on nanosized fillers for gas separation applications.

**WP4 “Functional Mesoscale Models for the Permeability of Smart Nano-porous Biomedical Materials for Biomaterial Applications”:** Here mainly atomistic and mesoscale simulations will be used to make CAMD contributions to the design of much improved gels for anti-fouling rigid contact lenses with high oxygen permeability to address the needs of the growing number of contact lens users.

Polymeric hydrogels represent a class of highly potent biomedical materials, and are well suited for a broad range of bio-applications, ranging from contact lenses to transport systems for drug delivery, due to the wide range of designer properties. Although this flexibility is very desired from a materials design point of view, the direct compound-structure-properties relation remains largely unknown, and poses important design challenges. Computational design approaches could steer the experimental design, by not only elucidating factors that are important for specific functionality but also by enabling the designer to control these properties in a rational way. True rational design however remains a challenge in (soft) nanotechnology, due to limitations on both sides: state-of-the-art *molecular* models are severely limited in system-size (time and space), and state-of-the-art *mesoscopic* models are only valid for rather homogeneous systems, due to the averaging procedures employed. The experimental reality is that systems are often both rather heterogeneous and ill defined, and that the resolution of the experimental characterization methods is severely limited. In WP4, we proposed to develop a rational design strategy for a high-impact biomedical application example (see furtheron) by an integrated approach of experiments and mesoscopic computations. On the computational side, existing mesoscopic models were found unfit or too inefficient for large-scale gel simulation, and new methodology had to be developed, implemented and tested in a consistent way. New state-of-the-art methods, a hybrid mesoscopic method (within the existing Culgi software package) and reactive dissipative particle dynamics (RDPD), have been developed during the past three years. The

experimental application example differs from the originally proposed contact lenses, but is of utmost importance for the development of another branch of biomedical research: targeted drug delivery. The proposed system, gel nanoparticles or *nanogels*, can serve as transport vehicles for bioactive molecules (e.g. drugs, proteins, RNA or DNA) for disease treatment (e.g. in cancer cells) as well as for imaging purposes. Nanogels have several advantages over more standard micelles or vesicles drug-delivery systems, in particular in terms of improved stability and designer properties.

The experimental design focussed on hydrogel synthesis and determination of structural and functional properties in both macro- and nanogeometry. Nanogels with four different monomers were selected based on simplicity and bio-compatibility: polyethylene glycol Methacrylate (PEGDMA), 2-Hydroxyethyl methacrylate (HEMA), Dextrane (T10)-(10%)HEMA (DEX-HEMA) and Arginine methacrylate ([Arg]nMA) (OEGDMA). Initially, the nanogels were prepared from monomer-rich reverse (water) micelles in an organic solvent, followed by a photopolymerization step and surfactant removal (see figure 1 for the nanogel synthesis pathway). Crosslink density and nanogel size could be controlled by varying the ratio of monomers and in the preparation of the reverse micelles, respectively. Due to very polydisperse nanogel dimensions, later preparation methods were liposome-mediated.

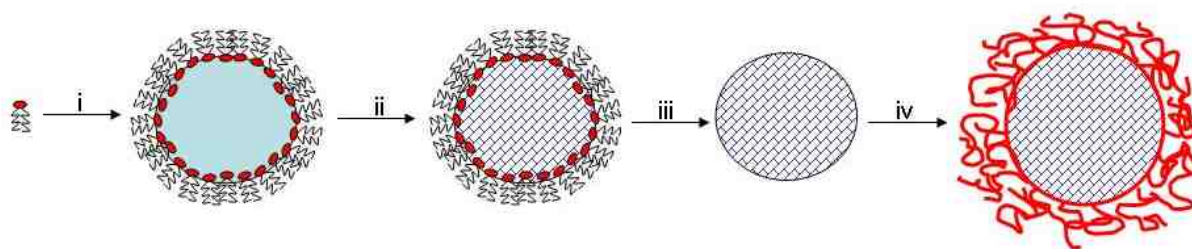


**Figure 1.** Original synthesis route of Nanogels. i) Mixing of AOT in a water/oil mixture results in monodisperse inverse micelles. The water phase contains a (photo)crosslinkable monomers and. ii) (Photo)polymerization transforms the aqueous phase into a hydrogel. iii) Removal of AOT if desired. iv) Surface-initiated polymerization of (meth)acrylates via ATRP or *N*-carboxy anhydride amino acids via a ring-opening polymerization. The entire process is compatible for sensitive (Bio)molecules like (DNA, oligonucleotides, proteins, etc), and encapsulation yields a nanocell with controlled diameter in the range of 10-50 nm.

The structural characteristics (mesh size) of unloaded gels were determined in detail by small angle neutron scattering (SANS) for both geometries. Most macrogels were found to be closed gels, with one characteristic length-scale in the order of 1-2 nm. The DEX-HEMA system shows the characteristics of an open gel with two characteristic sizes: 3.0 and 42 nm. For the nanogels, the low concentration of particles as well as limitations to the diffractometer resolution and measurement time did not allow for a determination of the mesh size, and only the monomer density profile, overall shape and characteristic size (also using DLS measurements) could be determined. For instance, for small DEX-HEMA nanogels (5 nm), both the inverse micelles and the nanogels were found to be non-spherical, or, alternatively, have a non-uniform core-corona-like structure. Also the release kinetics from and diffusion of several bio-active molecules (oligonucleotides, alanine) in the macrogel was measured in detail. The experimental method (pulsed field-gradient spin-echo NMR spectroscopy) is limited to diffusion at a structural level that is larger than the mesh size, thereby probing only effective values. Nevertheless, the resulting *effective* diffusion coefficient was shown to be sensitive to the particular gel structure, and in general severely reduced upon increasing monomer concentration. In addition, the swelling, yield, and stability of nanogels, DNA release rates, as well as toxicity and transfections (using HeLa cells) were considered for all nanogels. Transfection of HeLa cells with different nanogels revealed that small particles (30-110 nm) can successfully be used as a carrier for short interference RNA and DNA (figure 2).

The most efficient transfection is with a very compact polyacrylamide nanogel, where particles prefer to stay at the nucleus, but the toxicity of polyacrylamide (and radicals formed after destruction of the particle) gives rise to a short lifetime of the HeLa cells after transfection. The toxicity of the target nanogels was determined by a Cell proliferation assay method using HeLa cells, and shows that relative large concentrations (for DEX-HEMA 0.38 mg/ml) lead to little toxicity. To determine the dsDNA release rate and the encapsulation efficiency, double strand DNA was encapsulated in nanogels, including DEX-HEMA nanogels. A UV-absorption technique at different wavelengths shows that an encapsulation efficiency of 86.5% can be reached. DEX-HEMA is biodegradable for  $\text{pH} > 10$ .

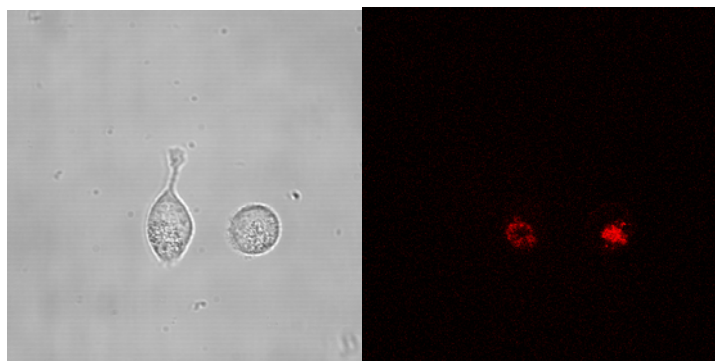


**Figure 2.** Transfection of DEX-HEMA nanogel in HeLa cells. The nanogels encapsulate oligonucleotides that are labeled with a fluorescent probe. The fluorescence indicates the presence of nanogel inside the HeLa cell.

In short, all experimental data point at DEX-HEMA nanogels as the target system for further study. Diffusion limited release seems insufficient for small nanogels, and release by using biodegradable gels and immobilized bio-active molecules is the most promising option. Details have not appeared in the literature due to patenting issues.

State-of-the-art methods for modeling structure-formation dynamics at the mesoscale were previously based on ‘pure’ particle- and field-based formulations, and unfit for modeling heterogeneous gel systems (based on methodological and/or efficiency restrictions). In this project, we formulated a new hybrid approach that enables the description of a system in a mixed formulation of interacting particles *and* fields, where fields describe the *abundant* constituents (solvents, surfactants) and particles the *sparse* components (gel network, permeant). The general concept is based on coupling different representations, and a merger of dynamic density functional theory (DDFT, describing the evolution of fields) and Brownian dynamics (BD, the same for particles) was implemented in the Culgi software package (see Figure 3, top, for an application example), including the effect of electrostatics (in Debye-Huckel formulation). The validity of this approach has been tested for a number of standard systems.

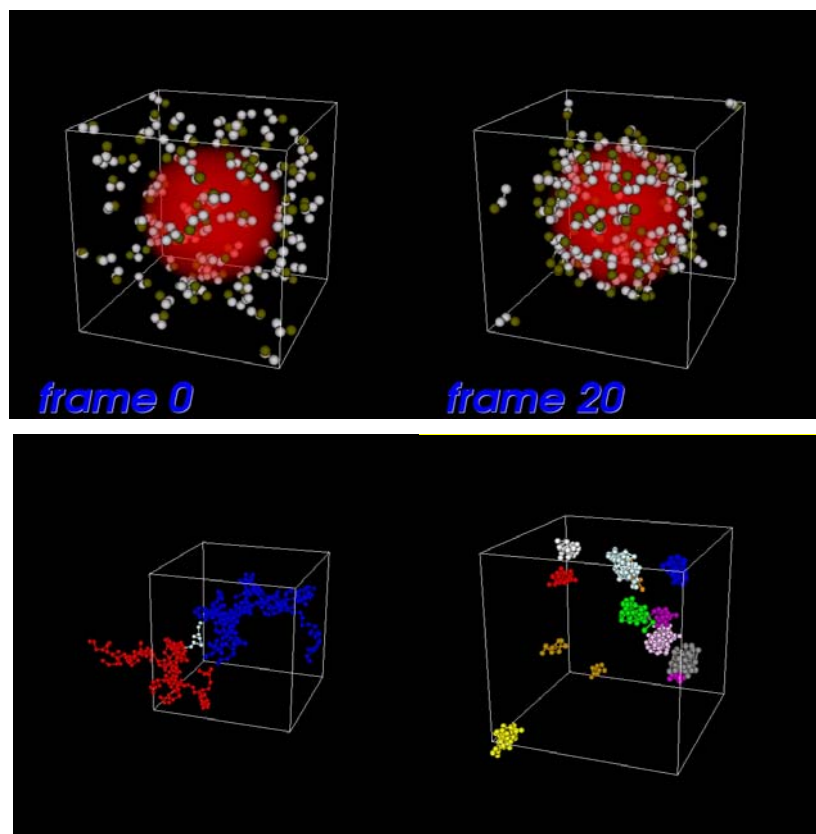


**Figure 3.** Top: Hybrid calculation for an oil droplet (field, red) surrounded by water (field, not shown) and surfactant molecules (particles, short chains). Left: initial configuration, with surfactant placed at random positions, right: later stage, where the surfactants assemble at the oil/water interface. Bottom: reactive DPD calculations (after 2000 timesteps) for equal initial (low) monomer concentration and good (left) and less good (right) solvent. For visualisation, the solvent is omitted in both images.

Effective permeability was determined as the most prominent characterization tool for the application example. We used the approach of Gusev, and solved the governing Laplace equation for the chemical potential on the existing computational grid in order to determine the effective permeability of small permeants. An advantage of this implementation is that the effective permeability can be calculated at run-time, for (arbitrary) complex mesostructures along the structure formation pathway. The local permeability is input as a field (and is a linear combination of permeability in the microdomains), but particle-to-field mappers can be used for the conversion of the particles. In addition, the hybrid model allows for the incorporation of so-called tracer particles in order to access the local and effective permeability by simulation.

Two basic computational studies were carried out to reveal details about the 3D gel microstructure and release rates. The relation between *hydrogel structure* and *small probe kinetics* was investigated by a BD method with implicit solvent. We considered two predefined networks, a regular diamond lattice (reference) and an inhomogeneous network (reflecting the gel network), and different degrees of swelling. The static structure factors as well as the mean squared displacement of small probes for different network structures and degree of swelling were determined, but not further analyzed due to the high computational efforts required. Instead, the *formation of a crosslinked network* (figure 3, bottom) was considered by adding reactions to an existing state-of-the-art self-consistent dissipated particle dynamics (DPD) formulation (originally developed by I. Pagonabarraga). In this method, DPD monomers can react to form a network structure, with connectivity depending on initial concentration and solvent quality, and this process can be monitored in time. The simulations

allowed for determination of both the percolation threshold and the fractal dimensions of the formed networks, and can, in combination with experimental SANS measurements, in the future be used to determine the fundamental fractal dimension vs characteristic length (mesh size) scaling relation. Both simulation studies provided additional information of the small-scale structure and phenomena that are beyond the experimental resolution, and are essential for the parameterization of the efficient hybrid method.

The use of the hybrid method for meaningful modeling of the experimental complex gel systems required proper choices of molecular, interaction and coupling parameters. The relation of the first two parameter sets and experimental conditions is known from earlier BD/DPD and DDFT studies. In this project, the manpower awarded to computational and theoretical work (the bulk of the budget was directed towards experimental work) was insufficient to completely fulfill the requirements for full parametrization. Nevertheless, the detailed experimental and computational results in WP4 are complementary and provide detailed insight in this complex system. This information will be explored for a full parametrization and validation of the hybrid method, but this goal is left for future work.

#### **Publications published and submitted so far:**

**G.J.A. Sevink** and A.V. Zvelindovsky, “Mesoscopic dynamics of complex vesicle formation: kinetic versus thermodynamic factors“ *Molecular Simulation* 33, 2007, 405-415.

**G.J.A. Sevink** and J.G.E.M. Fraaije, “Modelling complex systems in full detail: a new approach” in *AIP CP 982*, Ed. M. Tokuyama, 2008, 491-497.

**G.J.A. Sevink** and J.G.E.M. Fraaije, “Direct calculation of permeability in nano-structured block copolymers” submitted.

#### **Prospect for further use:**

The hybrid method is suited for modeling gel systems, but also represents a unique dynamic alternative for a static DFT/SCF model for nanocomposites, where (coated) functional nanocolloids are mixed with block copolymers to achieve new functional nano-materials. In the hybrid formulation, particles can be clustered to represent nano-colloids, and the methods efficiency is sufficient for large-scale simulations. Our group is internationally leading in the field of mesoscopic structure formation dynamics in block copolymers, and will exploit this new field in the future. A European proposal, aimed at designing crossbar motifs for microelectronics, has been submitted to the recent NanoSci-E+ call. The hybrid method is incorporated in the Culgi software package, owned by the small SME MesoDyn BV.

Functional nanogel carriers will be used (in-vivo) for medium/high throughput drug testing and discovery in zebrafish, in the context of a Dutch SmartMix project. Here, the focus is on osteoporosis/bone regeneration, which can be accessed by removing part of the caudal fin and insertion of nanogels directly into the wound.

**WP5 “Molecular modelling of degradation of biodegradable polymers”**: Mainly atomistic complemented with QM methods will be used to get a better basic insight in bio degradation processes and to eventually make CAMD contributions to the design of polymeric materials with tailor-made degradation properties.

#### **Description of background and key results**

Control over the degradation and erosion behaviour of hydrolytically degradable aliphatic polyesters is highly desired, especially for their applications in biomedicine and pharmacy. In

order to enable this control a thorough understanding of the basic phenomena involved in these processes is needed. In spite of the numerous experimental studies carried out in the last decades, essential information is still missing at a molecular level. This work package used a different and successful approach to get access to this information: the combination of computational simulations at two different scales, detailed atomistic molecular dynamics and quantum mechanical calculations. Since the hydrolytic erosion of these materials can be interpreted as a transport-reaction process, the mentioned combination of the two levels of simulation is a proper methodology to study the basic parameters governing the erosion process. The transport of water in the polymer is addressed using atomistic modeling, while quantum mechanical simulations are employed to study the hydrolytic cleavage of the ester bonds in the polymer backbone.

A group of poly( $\alpha$ -hydroxy esters) based on glycolic and lactic acid was selected for the investigation: two homopolymers, polyglycolide (PGA) and poly(L-lactide) (PLLA), two stereocopolymers, poly(rac-lactide): PLA<sub>50</sub> and PLA<sub>96</sub><sup>1</sup>, two copolymers, poly[(L-lactide)-coglycolide]: PLA<sub>73</sub>GA<sub>27</sub> and PLA<sub>82</sub>GA<sub>18</sub> and poly[(rac-lactide)-co-glycolide], PLA<sub>36.5</sub>GA<sub>27</sub>. This selection allows to examine the effect of the polymer composition (glycolyl, L-lactyl and D-lactyl units contents) on the erosion behavior of the materials. Furthermore, a slow degrading polycarbonate ester not belonging to this family, poly(1,3-trimethylene carbonate), PTMC, was included in the study. The respective repeat units are displayed in figure 5.1.

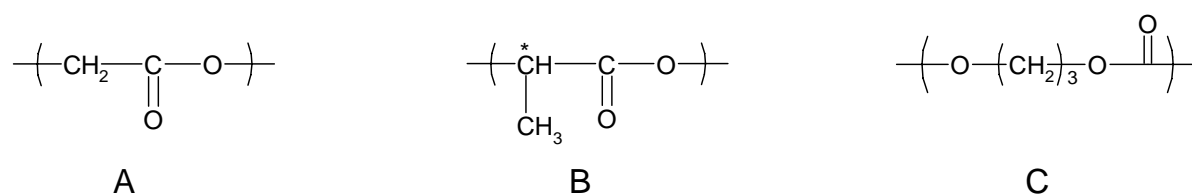
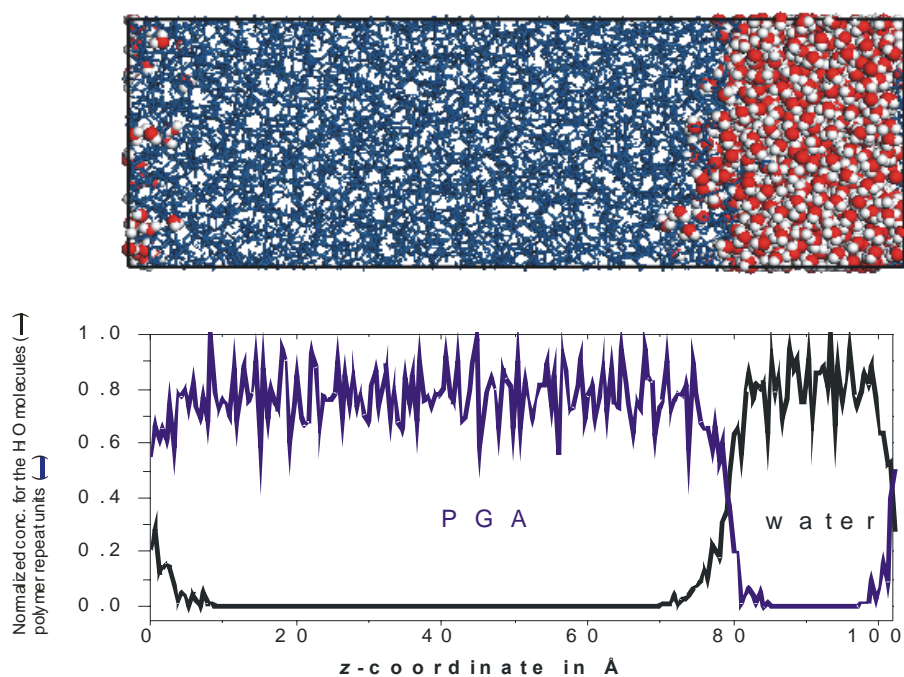


**Fig. 5.1:** Repeating units for glycolic acid (A), lactic acid (B) and trimethylene carbonate (C).

Atomistic bulk models for the homopolyesters using two different forcefields —COMPASS forcefield and a modified PCFF— were analyzed and evaluated. The modified PCFF was the forcefield giving the best results when compared with experimental data, and thus it was selected for the study. Atomistic bulk models using this forcefield were generated for the chosen polymers. The models were equilibrated and validated by comparison with experimentally obtained data (e.g. values of density, X-ray scattering curves) and with quantum chemical calculated properties (e.g. torsional energetics). Two more sets of bulk models were constructed for hydrated systems: polyesters containing approximately 2% and 7% of water contents in weight. These models were also sufficiently equilibrated and later subjected to systematic molecular dynamic simulation in order to obtain long trajectories for the production of data. Afterwards, the systems were thoroughly analyzed concerning several properties connected to the permeation of water through the materials, the influence of hydration on the polyesters and the different interaction of the systems with water. Some of the calculated properties are free volume and mobility of the polymeric chains, diffusion of water, affinity of the matrices for water in terms of solubility parameters and self-aggregation of water molecules and volumetric swelling undergone by the models.

<sup>1</sup> Nomenclature: PLA<sub>x</sub>GA<sub>y</sub> with X= % in weight of L-lactyl units, ((100-X) = % D-lactic unit and Y = % in weight of glycolic units.

(A)



(B)

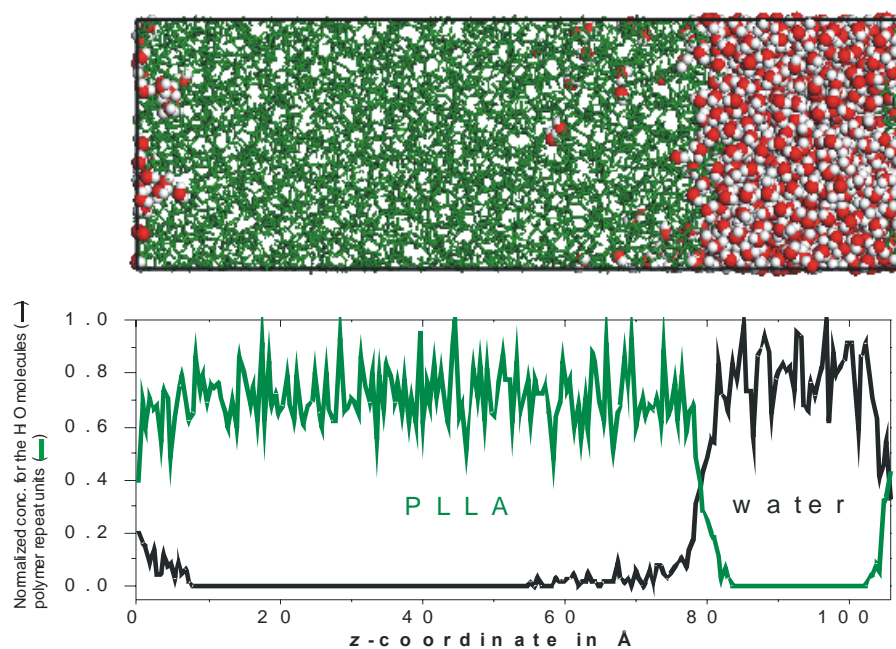


**Fig. 5.1:** Interface between PGA (blue) and water (red and white) (a) and between PLLA (green) and water (red and white) (b) after 4 ns of MD simulation. Below the snapshots, the normalized concentration profiles for the polymers and for water are shown.

In addition, atomistic interface models were constructed for the homopolyesters in order to get a better insight into the first moments of contact between the polymers and water. This simulations show that at these short times only few molecules managed to penetrate the polymeric matrixes. Once the molecules have penetrated the systems, they travelled faster in PLLA than in PGA (cf. Figure 5.1). This is in agreement with the higher diffusivities of water found in the bulk models simulations for PLLA compared to PGA.

For the homopolymers, it was found that the higher experimentally observed water uptake undergone by polyglycolide in comparison to poly(L-lactide) is caused by a higher solubility of water in polyglycolide than poly(L-lactide), which overcompensates by a large extent the higher diffusivity of water through poly(L-lactide). This higher solubility is related with the higher density of polar groups existing in polyglycolide due to the absence of the methyl group that poly(L-lactide) has as a side chain.

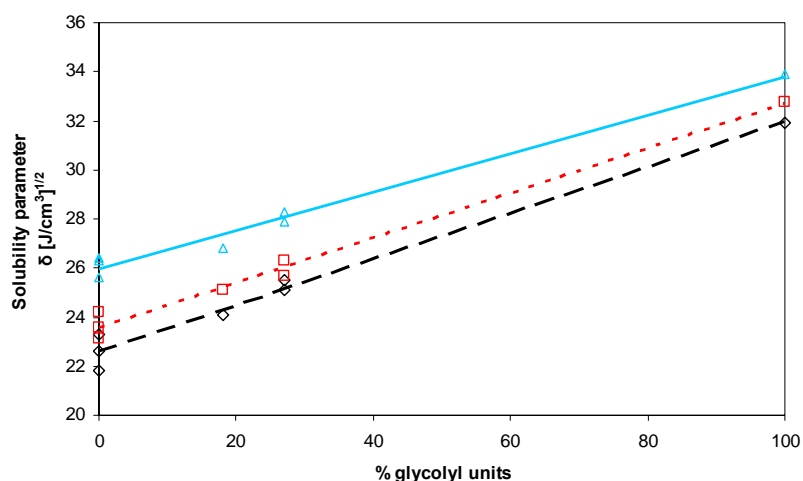


**Fig. 5.2:** Solubility coefficient as a function of the percentage of glycolyl units.

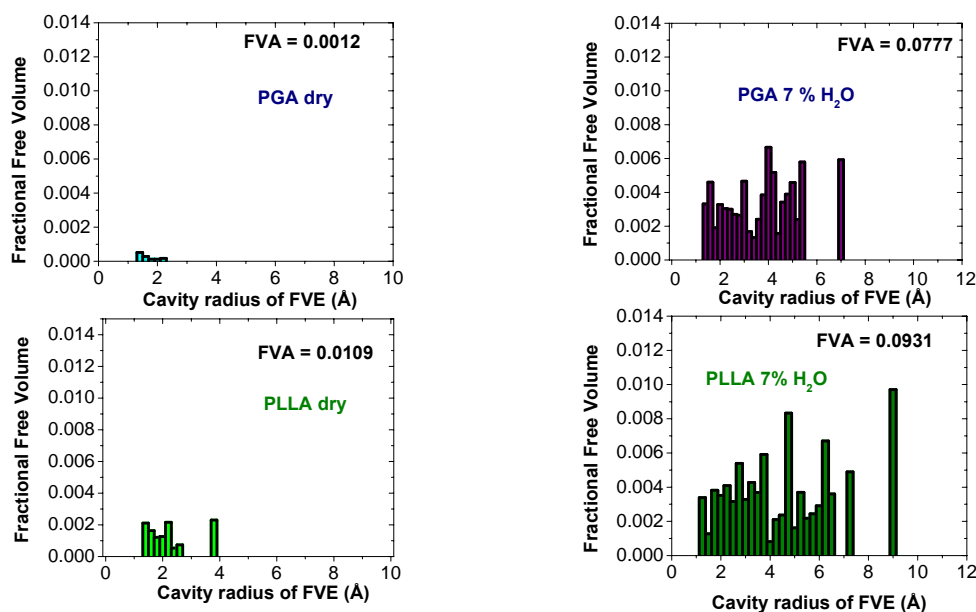


**Fig. 5.3:** Fractional free volume accessible for water for PLLA and PGA in the dry state and in the hydrated systems (the water molecules were removed prior to the calculation of the free volume).

Several of the studied properties showed strong correlation with the percentage of glycolic acid units present in the polymer, e.g. the solubility parameter, the volumetric swelling or the increase in free volume with hydration (see Figures 5.2 and 5.3). In general, the glycolyl units also exhibited stronger interaction with water.

Furthermore, the simulated systems confirmed the experimentally indicated self-aggregation of water in the systems. For all the polyesters studied, water molecules tend to form clusters in the bulk of the polymer. In the less water-swollen models, water molecules diffuse on average in couples, while in the models with 7% of water contents in weight, water forms clusters of three molecules on average (see Figure 5.4).

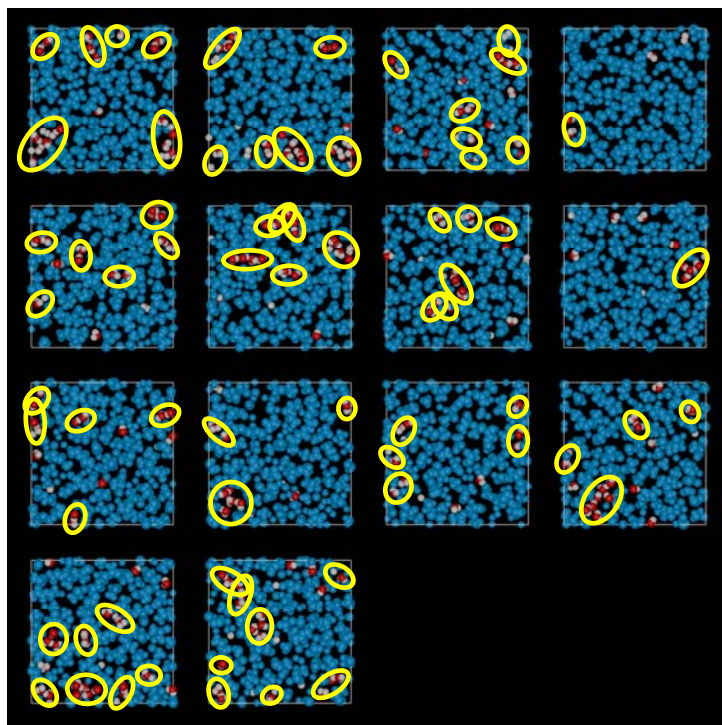


**Fig. 5.4:** Illustration of the formation of water cluster in PLA<sub>50</sub> 7% H<sub>2</sub>O.

The quantum chemical study of the hydrolysis of oligomers constituted of three ester units, GG (related with PGA), LL-1, LL2 (related with PLLA), LD-2 (related with the lactic acid stereocopolymer and TMC (related with PTMC), was investigated for the neutral water-assisted hydrolysis—involving two water molecules, one of the molecules acting as a nucleophile and the second one catalyzing the reaction. It was carried out at two different levels of theory: HF/6-31G\* and B3LYP/6-31G\*. It revealed a more favourable scission of the glycolyl units than of the lactyl units, with a lower energy barrier due to both electronic and steric effects of the extra methyl group existing in lactic acid units. The hydrolysis is also slower for TMC, in this case due only to electronic effects.

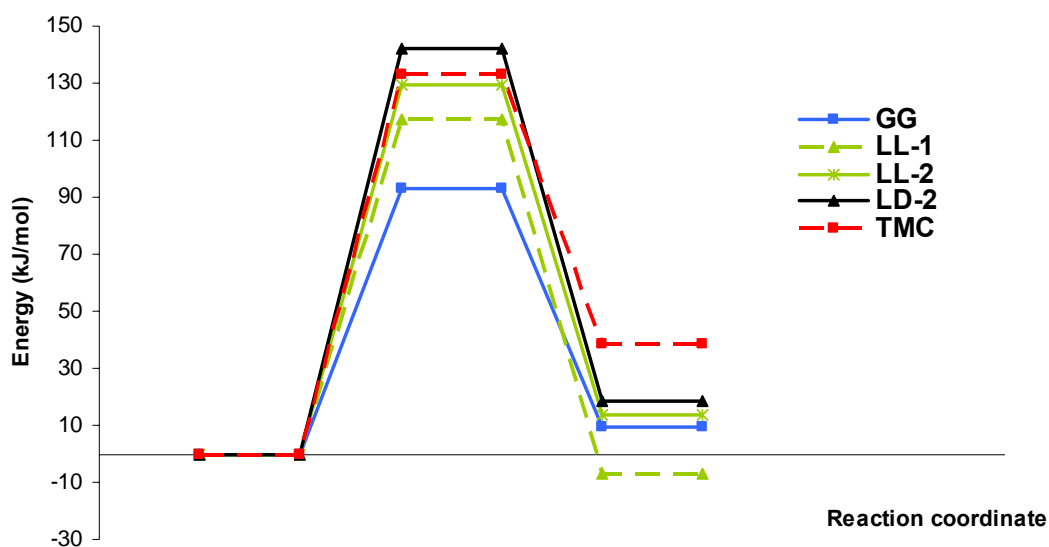


**Fig. 5.5:** Energy profile for the first step of the hydrolysis at B3LYP/6-31G\* computational level.

Finally, the results from the two different scale investigations were discussed together and related to the results from experimental studies. A better understanding of the basic phenomena involved in the hydrolytic degradation and erosion of poly( $\alpha$ -hydroxy esters) was achieved.

#### **Publications submitted so far:**

M. Entrialgo-Castaño, A. Lendlein, D. Hofmann, *Advanced Eng. Mat.* **2006**, 8, 434-439  
 M. Entrialgo-Castaño, PhD Thesis, GKSS, **2007**.  
 M. Entrialgo-Castaño, A. Lendlein, D. Hofmann, *Macromol. Symp.*, **2008**, *in press*.

#### **Prospect for further use:**

During the project the knowledge generated has been sufficient to now extend the investigations systematically (with GKSS funds) and to combine them with respective experimental studies. The aim is to now routinely utilize CAMD at GKSS as a tool for the development of new biomaterials with tailored hydrolytic degradability.

**WP6 “Coordinated experimental investigation and computer simulation of the functioning of simple monolithic controlled release devices”:** Parallel experimental investigation and computer simulation of the functioning of polymer-based, solvent-activated, matrix-type, controlled release (MCR) devices; The results are expected to promote the use of computer simulation as a valuable tool for optimum design of commercial MCR (and similar biomedical) devices and to help establish computer-assisted evaluation of end-use performance as a valuable complement of CAMD of polymeric materials. These results should contribute to new developments in a highly attractive market of tens of billions of Euro per year.

#### **Description of background and key results**

The need to deliver drugs, agrochemicals or other bioactive agents in regulated doses has led to rapidly increasing interest in the design and use of controlled release devices. Matrix controlled

release (MCR) devices consist of a swellable polymer matrix incorporating the requisite bioactive solute, and are activated by the ingress of water when placed in an aqueous environment. Their structural simplicity and ensuing low cost of manufacture account for their wide (and rapidly growing) practical use. Nevertheless, MCR devices are commonly characterised by a continuous decline of dose rate, which is particularly marked in the initial stages and constitutes a substantial drawback for most practical applications. Accordingly, optimum design of CR devices of the above type requires not only (i) achievement of a delivery rate within specified limits (known in drug delivery as the "therapeutic range"), but also (ii) maximisation of the efficiency of the delivery, i.e. of the fractional amount of embedded solute which can be delivered within these limits.

Evaluation of the aforesaid efficiency obviously requires detailed knowledge of the kinetics of solute release. Thus, a computer model which can simulate realistically the (strongly interacting) fluxes of invading water and exiting solute in MCR systems (and hence predict the resulting rate and kinetics of release) can serve as a valuable tool for the design optimization of such devices.

In this respect, within the framework of WP6, the following two main lines of research were pursued:

- (a) development of a macroscopic model simulating the functioning of multilayered, MCR devices and performance of generic parametric studies in order to determine to what extent the problems of non-uniformity of dose rate and initial burst effect, which normally characterize monolithic (single-layer) MCR devices, may be alleviated by the use of multilaminate devices
- (b) detailed validation of model against experiment, by generation of experimental solute release and other supplementary data specially designed to parameterize and test various aspects of the above computer models.

*In relation to objective (a)*, the model developed, applicable to planar, symmetrical three-layer (ABA) MCR devices of thickness  $2L$  (Fig. 1), is based on our previous model for single-layer systems [J.H. Petropoulos et al., J. Polym. Sci., Part B: Polym. Phys., 30 (1992) 717]. It accounts explicitly for transport of both solvent—usually water—and solute (denoted by subscripts W and N, respectively) as well as the interdependence of those two processes.

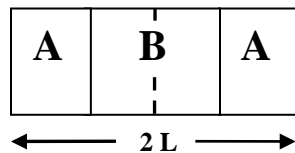


Fig. 1. Schematic presentation of a three-layer, ABA, device of thickness  $2L$ . Due to symmetry, the device is represented by two layers of total thickness  $L$  ( $L_A + L_B/2 = L$ ).

The parametric study included, three-layer ABA systems with

- (a) *unsaturated* (initial concentration of the solute in the matrix,  $C_{N0}$ , lower than the saturation value for the concentration of mobile solute in the fully hydrated polymer,  $C_{NS}^0$ ) and
- (b) *supersaturated* ( $C_{N0} > C_{NS}^0$ ), inner and outer layers.

For both categories the cases of

- (i) *fast water penetration* (ratio of diffusion coefficient of solute in the fully hydrated matrix to the diffusion coefficient of water,  $D_{NE} [= D_{NE}/D_{WA}] = 0.1$  or  $0.01$ ) and of
  - (ii) *comparable rates of solute and water diffusion* ( $D_{NEA} = 1$ )
- have been studied.

The effect of varying *solute loading*  $C_{N0B}$  (example shown in Fig. 2) or the *permeation properties* of the polymer ( $D_{NEB}$ ,  $D_{WB}$ ,  $C_{WB}^0$ ,  $C_{NSB}^0$ , example shown in Fig. 3) in the inner layer B, as well as of varying the *relative thickness* of the layers ( $L_A/L$ ), were examined in a systematic way.

The results has led to useful guidelines for the optimization of MCR devices and has revealed important possibilities of markedly improved performance by the use of ABA matrices in both the uniformity of release rate and the reduction of the burst effect, in comparison with the corresponding single-layer A devices, serving as benchmark here. In particular,

- in the case of uniform permeation properties, substantial improvement is predicted to be achievable with ABA-MCR devices characterized by (i) highly loaded-supersaturated B layers (with  $L_A/L_B \sim 1$ ), in cases of fast solvent penetration (where monolithic MCR performance is at its worst), as well as in cases of comparable solvent-solvent transport rates (where monolithic MCR performance is not too unsatisfactory) as exemplified by green lines in Figs. 2; (ii) unsaturated B layers, in the case of comparable solute-solvent transport rates, provided that  $L_A \ll L_B$  (e.g. red dash-dotted lines in Figs. 2).

- in general, supersaturated matrices offer greater possibilities for all-round improvement of the performance than unsaturated ones, and  $C_{NO}$  is more effective in manipulating the burst effect than  $D_{NE}$ , while  $D_{NE}$  is effective in manipulating the release rate (e.g. blue and red lines in Figs. 3)
- the osmotic action of the solute may prove beneficial in cases of inferior MCR performance but is likely to be deleterious in instances of good performance. In any case, the said effects cannot be ignored in ABA, as well in monolithic, MCR design.
- finally, the ABA model presented here, can simulate the performance of practical, transdermal patches or similar MCR devices, but can also offer a useful approximation to commercial coated tablets (e.g. Fig. 3).

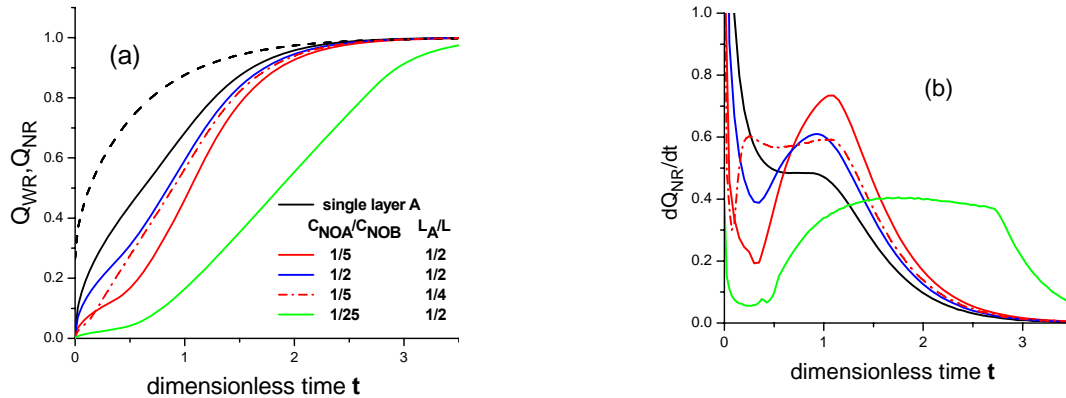


Fig 2. *Example of predicted release performance by three-layer ABA matrices with uniform permeation properties and distributed solute load,  $C_{NO}$* : (a) Computed solute release kinetics from reference single-layer (—) and from three-layer (colored lines) matrices and concurrent water uptake (---);  $C_{NSA}^0 = C_{NSB}^0 = 5$ ;  $D_{NEA} = D_{NEB} = 1$ . (b) Results of Fig 2a plotted in terms of fractional solute release rate  $dQ_{NR}/dt$ , showing more clearly the uniformity of rate achieved in each case. Notation as in Fig. 2a.

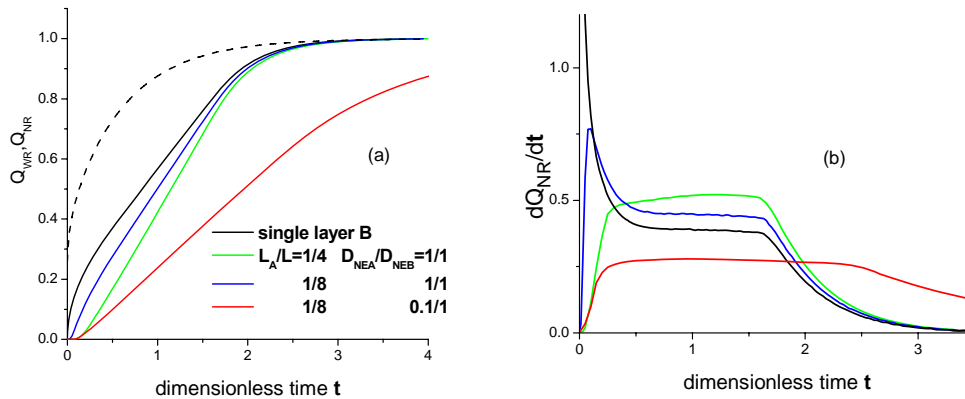


Fig 3. *Example of predicted release performance by three-layer ABA matrices with distributed permeation properties and solute-free outer A layers (approximating commercial coated tablets)*. (a) Computed solute release kinetics from reference single-layer B (—) and from coated (colored lines) matrices and concurrent water uptake (---).  $C_{NSA}^0 = C_{NSB}^0 = 5$ ;  $C_{NOB} = 10$ ,  $C_{NOA} = 0$ . (b) Results of Fig. 3a plotted in terms of fractional solute release rate  $dQ_{NR}/dt$ . Notation as in Fig. 3a.

*In relation to objective (b) :*

The methodology adopted for testing the MCR model was to (i) first determine, by independent measurements the sorption and diffusion properties of the experimental system cellulose acetate (polymer)-water (solvent)- NaI (solute) (ii) then use the resulting experimental data to parameterize

the relevant computer model and simulate the behavior of MCR devices based on the said system under various conditions, and (iii) compare the simulated behavior with the corresponding experimental release performance of cellulose acetate-based MCR devices.

The system cellulose acetate (CA)-H<sub>2</sub>O- NaI was specially chosen for testing certain critical features of the relevant model, such as adequate representation of a solute-induced osmotic effect. Loading of cellulose acetate (CA) thin films, was achieved either by equilibrating the neat films with aqueous solutions of NaI of various concentrations (type A films) or by introducing the NaI at the film preparation stage by dissolving an appropriate amount of NaI in the acetone dope (type B films). Characterization of the sorption and diffusion properties of the system CA-H<sub>2</sub>O-NaI, included

- the water vapor isotherm, as well as the effect of NaI loading on water uptake (osmotic effect) ,
- the diffusion coefficient of water in CA, by analysis of the non-Fickian kinetics of liquid water uptake in neat CA films, on the basis of our previously developed model [K. Papadokostaki et al. J. Polym. Sci. Polym. Phys. 40 (2002) 1171] accounting for the structural relaxation of the swelling glassy polymer matrix,
- the dependence of partition coefficient of NaI on the water content of the polymer as well as on the NaI loading, and
- the dependence of the diffusion coefficient of NaI on the concentration of imbibed water in the film (Fig. 4)

The experimental release performance of CA-based devices was determined as a function of NaI loading and initial water activity. For a more exact testing of the model, the water uptake kinetics, during the release process, were also monitored (e.g. Fig. 5). The results indicate that the method of loading (type A or type B matrices) has no effect on the kinetic behaviour of the device. Thus, as shown in the example of Fig. 5, with increasing NaI load, C<sub>NO</sub> (i) the maximum in fractional water uptake, Q<sub>WR</sub>, in the matrix, increases due to the intensification of NaI's osmotic effect, (ii) the rate of fractional amount of solute released, Q<sub>NR</sub>, increases and (iii) deviation from  $\sqrt{t}$  release kinetics becomes less marked. Comparison of the simulated and experimental behavior, indicates that the model captures well all the main features of the experimental data pertaining to both the fractional water uptake and the fractional solute release kinetics (e.g. Fig. 5).

Thus, the above work provided a successful detailed validation of the model against experiment. The results demonstrate the practical applicability of our model and the usefulness of computer simulation as an important tool for the rational design of MCR devices exhibiting complex kinetic behaviour.

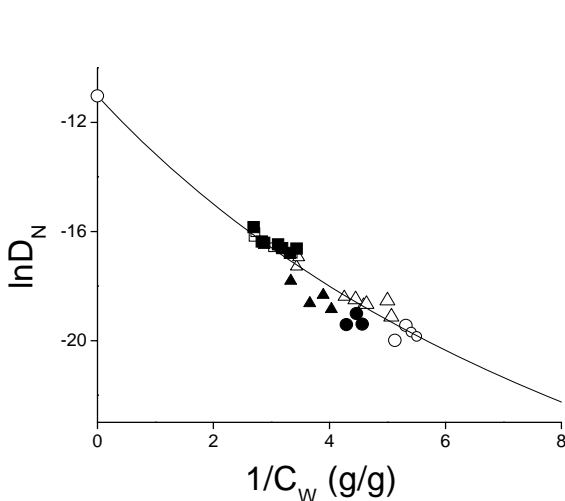


Fig. 4. *Example of determination of diffusion properties of the experimental system by independent measurements:*

Dependence of NaI diffusion coefficient,  $D_N$ , on the degree of hydration,  $C_W$ , of CA, determined from data on type A (open points) and B (filled points) films, equilibrated with NaI solutions of concentration (g/cm<sup>3</sup>) = 0.05 (○), 0.20 (△) and

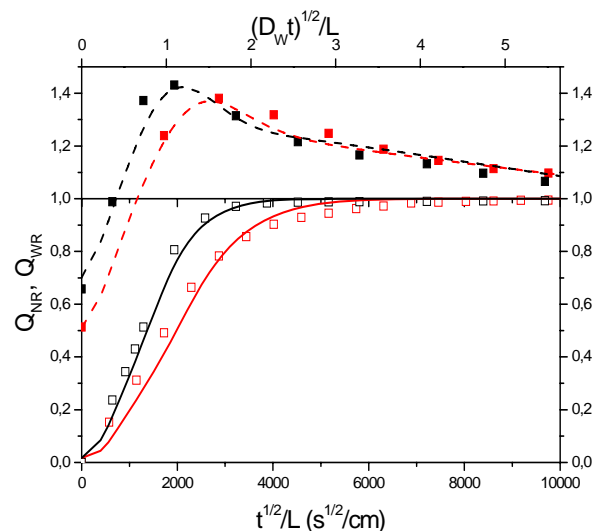


Fig. 5. *Example of testing the model against experiment:* Comparison of dimensionless computed NaI release (continuous lines) and water uptake (dashed lines) curves with experimental data (points) pertaining to type B matrices with initial NaI loading  $C_{NO}$  (g/g of dry polymer) 0.33 (black points and lines), 0.20 (red points and lines); initial water activity = 0.4.

0.40 (□). The line represents fitting to the relevant model equation, which was then used to parameterize the model and compute the release performance of the system (see example in Fig. 5)

Two PhD students, A. Stavropoulou, MSc Chemistry, and D. Soulas, MSc Chemistry, as well as a part-time, post-doc researcher, D. Spyriouni, PhD, Chemical Engineer were engaged under contract for the above described work, performed in WP6.

#### **Publications submitted so far:**

1. Papadokostaki, K.G.; Stavropoulou, A.; Sanopoulou, M.; Petropoulos, J.H. “A Model for the Prediction of the Performance of Multilayered Polymeric Matrix-Controlled Release Devices”, *Desalination*, **2006**,199, 441.
2. Stavropoulou, A. “Experimental and theoretical investigation of polymeric controlled release matrices”, PhD Thesis, Univ. of Athens, 2006
3. Papadokostaki, K.G.; Stavropoulou, A.; Sanopoulou, M.; Petropoulos, J.H. “An advanced model for composite planar three-layer matrix-controlled release devices. Part I. Devices of uniform material properties and non-uniform solute load” *J. Membrane Sci*, **2008**, 312, 193.

#### **Prospect for further use:**

The results obtained during the project, in relation to the capability of the model to simulate single-layer MCR devices of complex kinetic behaviour, are quite satisfactory to allow us propose its parameterization on the basis of CAMD calculations. In this way a fully computerised hierarchical modelling procedure can be applied, extending from simulation of the molecular structure of a given polymeric material right through to evaluation of its real-life end-use performance as a MCR device.

On the other hand, the parametric study performed, has revealed important possibilities of markedly improved performance by the use of three-layer MCR matrices. Thus, it is of practical importance to proceed to validation of this model too, by applying the methodology used in the project for the case of single-layer devices. In this respect, some relevant preliminary results presented in the 3<sup>rd</sup> year activity report, are quite encouraging.

Finally, our MCR modeling approach may be further developed for the case of biodegradation-, and/or dissolution-, controlled polymeric matrices.

#### **WP7 “CAMD and experimental characterisation of polymer / polymer composites for applications in life science and technical separation processes”:**

**Task 7.1:** CAMD and experimental contributions were used with the final goal of designing polymer/biopolymer blends with tailor-made biocompatibility. In particular three blends were investigated, each with three different weight ratios (80-20, 60-40, 40-60), considering diffusion and biocompatibility properties.

##### **Description of background and key results**

The combination of natural macromolecules with synthetic polymer materials to produce “hybrid” materials has become the object of increasing interest in recent years for the potentiality that these materials have for different applications, including biomedical ones (Giusti et al., 1994; Giusti et al., 1996 and Cristalli et al., 2001). Indeed, such materials, if obtained from a proper combination of synthetic polymer and biopolymer, should have enhanced mechanical properties, thanks to the synthetic component, and superior biocompatibility due to the biological one. Moreover, by setting the content ratio of the two components other properties of the final material, such as permeability, can be tuned. However, the mentioned experimental findings are not supported by a strong rationale, which would be the key to designing new materials based on properties prediction.

Concerning the natural part, several advantages can derive from the use of polysaccharides, first of all, because of the chemical similarities with heparin, polysaccharides show good hemocompatibility properties. Moreover they are non-toxic and have low costs in comparison with others biopolymers such as collagen. It was also observed that when they are blended with synthetic polymers they are able to exert a stiffening effect improving the mechanical properties of the produced materials (Cascone et al. 2002).

In this WP chitosan and dextran were selected as feasible natural part and were mixed with two synthetic polymers: polyvinyl alcohol (PVA), which is widely used due to its biocompatibility and chemical versatility, and polyacrylic acid PAA, which is one of the most important polyacids used for biomedical applications (Greenberg et al., 1978). Three hybrid materials, or blends, were considered in particular: PAA-dextran and PVA-chitosan, and PVA-dextran. Focus was put on their application as hemodialysis membranes or as drug delivery systems and, thus, on their mechanical characteristics and diffusion properties with respect to target molecules of interest.

In order to assess possible relationships between their chemical structure and their macroscopic physico-chemical properties the three blends were at the molecular level by means of computational models based on molecular dynamics (MD) and at the mesoscale level through models based on dissipative particle dynamics (DPD). The computational activity was paired with an experimental one. The latter was first performed to obtain preliminary indications and input data (i.e. water uptake and density) for subsequent computational activities and then provided output data (e.g. permeability coefficients) to validate computational outcomes.

Preliminary experimental tests showed that the PVA-Dextran blend was unstable in water solution. The computational study was thus focused on PVA-Chitosan and PAA-Dextran. Bulk amorphous, cubic, periodic cells of the blends in water-swollen conditions were implemented and refined for three polymer-biopolymer weight ratio: 80:20, 60:40, 40:60 (as exemplified in figure 7.1). Each model contained 6000÷8000 atoms and reflected the actual density and swelling of the material, as well as the conformation and tacticity properties of the polymers. For every model the material's Young modulus along the principal three principal directions of the periodic cell were estimated. They ranged from 5.22 to 6.22 GPa for the PAA-Dextran blends and from 3.64 to 3.79 GPa for the PVA-Chitosan ones, showing an approximately isotropic behaviour.

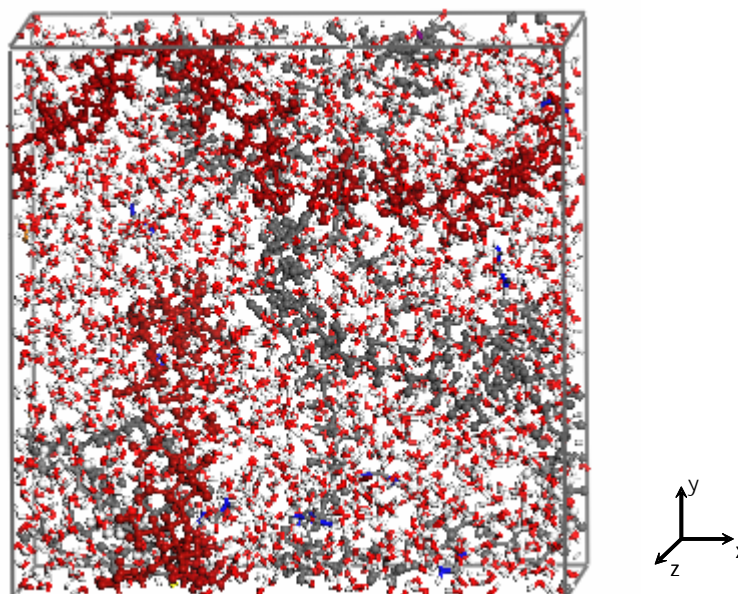


Figure 7.1 - PAA-Dextran 40:60 (w/w) bulk model after refinement procedure.

Diffusion and solubility constants (D and S) with respect to water and urea were also assessed. D was calculated by means of the Einstein equation from the mean square displacement of the permeant molecules. S was computed via the Widom test method, which was modified in order to be used for a planar and relatively big molecule as urea. Materials' permeability P was calculated as D·S. The obtained values are summarized in table 7.1.

Blend	S	D [cm <sup>2</sup> /s]	P [cm <sup>2</sup> /s]
<b>To water</b>			
PAA-Dextran 40-60	1.7244	2.01E-05	3.47E-05
PAA-Dextran 60-40	2.3804	3.22E-05	7.65E-05
PAA-Dextran 80-20	2.6136	3.52E-05	9.21E-05
PVA-Chitosan 40-60	1.6978	2.39E-05	4.06E-05
PVA-Chitosan 60-40	1.8247	3.19E-05	5.82E-05
PVA-Chitosan 80-20	2.1521	4.40E-05	9.48E-05
<b>To urea</b>			
PAA-Dextran 40-60	1.78E-17	4.23E-08	7.52E-25
PAA-Dextran 60-40	4.39E-16	5.84E-08	2.56E-23
PAA-Dextran 80-20	1.47E-17	8.70E-08	1.28E-24
PVA-Chitosan 40-60	1.04E-17	1.62E-07	1.68E-24
PVA-Chitosan 60-40	2.54E-18	9.56E-08	2.43E-25
PVA-Chitosan 80-20	1.43E-18	1.06E-07	1.52E-25

Table 7.1 – Solubility, diffusion and permeability constants calculated via MD modelling.

Computationally calculated permeability coefficients to water were compared to experimental values gathered on membranes samples of known characteristics for both blends. The same comparison was done only for PAA-Dextran with respect to urea diffusion (table 7.2). Good agreement was found and the MD models were thus considered validated.

Blend	P <sub>experiments</sub> [cm <sup>2</sup> /s]	P <sub>MDmodels</sub> [cm <sup>2</sup> /s]	D <sub>experiments</sub> [cm <sup>2</sup> /s]	D <sub>MDmodels</sub> [cm <sup>2</sup> /s]
PAA-Dextran 40-60	*	3.47E-05	5.46E-09	1.62E-07
PAA-Dextran 60-40	8.03E-06	7.65E-05	2.93E-08	9.56E-08
PAA-Dextran 80-20	3.18E-06	9.21E-05	6.13E-08	1.06E-07
PVA-Chitosan 40-60	3.77E-06	4.06E-05		
PVA-Chitosan 60-40	4.58E-06	5.84E-05		
PVA-Chitosan 80-20	4.75E-06	9.48E-05		

Table 7.2 – Comparison between experimental and computational values of permeability constants with respect to water and of diffusion coefficient with respect to urea.

The outcomes from MD simulations were qualitatively confirmed by the preliminary results obtained through coarse grain models based on DPD method.

Along with experiments aimed at evaluating the transport properties of the analysed materials, *in vitro* cytotoxicity tests were performed to assess their biocompatibility. PAA-Dextran and PVA-Chitosan with 3 different concentration 80:20, 60:40, 40:60 were considered. Tests were

performed using murine line fibroblasts on sterile samples and in controlled conditions. Periods of cells-sample interaction of 1, 3 and 7 days were considered. At the end of each timeframe cells were suspended with a proper medium and at 1 hour after sowing, their adhesion was observed. 1 ml of eluate was then added to each sample and left in contact with the cells for 24 and 72 hours at the end of which a biochemical Alamar Blue test was performed to assess cells vitality and observation by optical microscope was done.

<b>Polymeric material</b>	<b>1 day</b>	<b>3 days</b>	<b>7 days</b>
<b>Alamar Blue test after 24 hour of incubation.</b>			
PVA-Chitosan 80-20	0.786 ± 0.057	0.789 ± 0.033	0.818 ± 0.042
PVA-Chitosan 60-40	0.782 ± 0.052	0.802 ± 0.034	0.810 ± 0.044
PVA-Chitosan 40-60	0.800 ± 0.054	0.814 ± 0.039	0.794 ± 0.050
PAA-Dextran 80-20	0.791 ± 0.074	0.779 ± 0.048	0.771 ± 0.068
PAA-Dextran 60-40	0.776 ± 0.062	0.779 ± 0.018	0.706 ± 0.026
PAA-Dextran 40-60	0.826 ± 0.105	0.752 ± 0.017	0.705 ± 0.020
control	0.930 ± 0.032	0.930 ± 0.032	0.930 ± 0.032
<b>Alamar Blue test after 72 hour of incubation (ads 570 nm)</b>			
PVA-Chitosan 80-20	0.943 ± 0.034	0.905 ± 0.015	0.955 ± 0.018
PVA-Chitosan 60-40	0.950 ± 0.049	0.897 ± 0.021	0.934 ± 0.041
PVA-Chitosan 40-60	0.946 ± 0.033	0.937 ± 0.027	0.938 ± 0.022
PAA-Dextran 80-20	0.902 ± 0.033	0.904 ± 0.021	0.918 ± 0.028
PAA-Dextran 60-40	0.876 ± 0.035	0.918 ± 0.036	0.908 ± 0.040
PAA-Dextran 40-60	0.913 ± 0.028	0.893 ± 0.027	0.924 ± 0.034
control	0.930 ± 0.032	0.930 ± 0.032	0.930 ± 0.032

*Table 1 - Results of Alamar Blue tests, performed on elutes after 24 and 72 hours from cells culture (mean±standard deviation).*

All samples showed a similar behaviour and appeared to be biocompatible: similar quantities of Alamar Blue were reduced by the cells on all samples (table 7.3) and optical observation confirmed this result (figure 7.2).

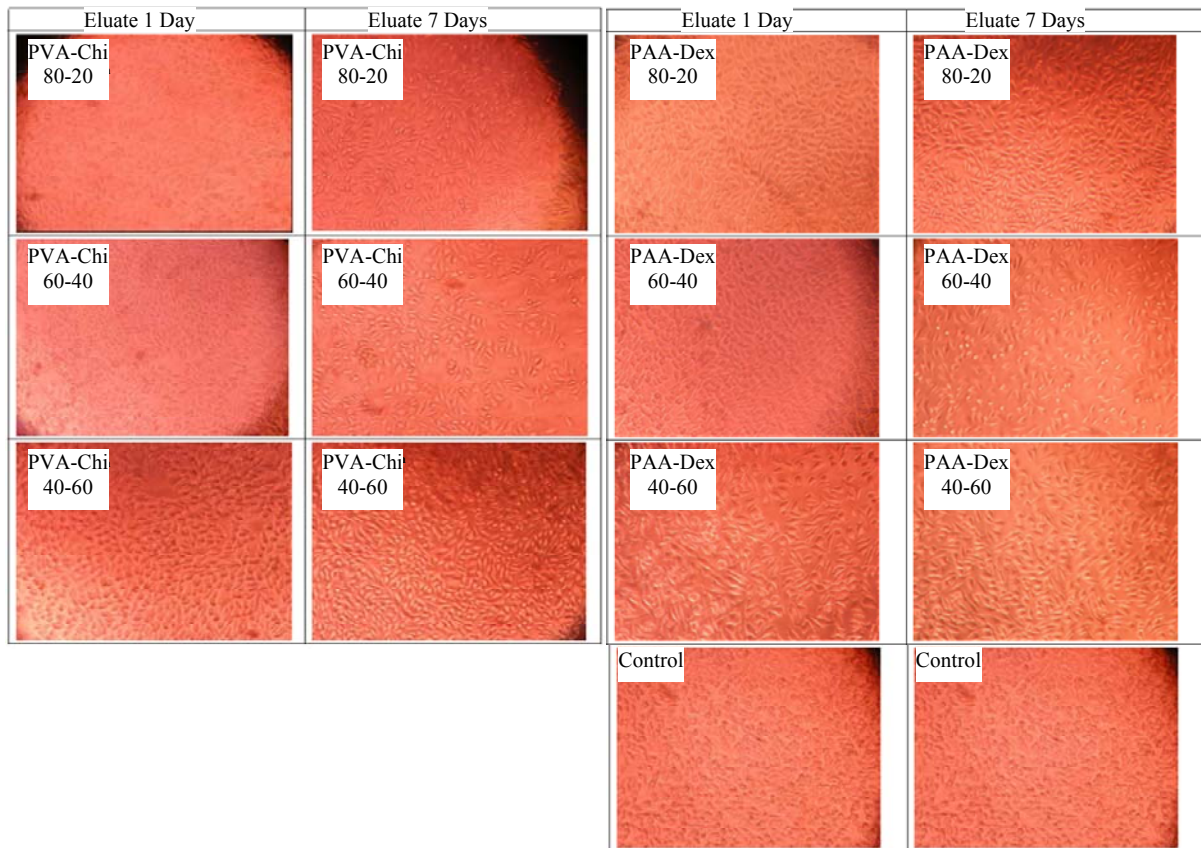


Figure 7.2 – Optical microscopy images of line fibroblasts remained in contact with eluates for 24 and 72 hours.

**Publications submitted so far:**

Ionita M., Silvestri D., Gautieri A., Votta E., Ciardelli G., Redaelli A., Desalination, Volume 200, 1-3 Pp. 157-159, 2006.

Ciardelli C., Silvestri D., Barbani N., Ionita M., Redaelli A., Giusti P., Desalination, Vol. 200, 1-3, Pp. 493-495, 2006.

Ionita M., Silvestri D., Gautieri A., Votta E., Ciardelli G., Redaelli A., Proceedings of ESDA 2006, 8th Biennial ASME Conference on Engineering Systems Design and Analysis Torino, Italy, Pages 1-10, July 4-7, 2006.

Ionita M., Gautieri A., Votta E., Redaelli A., Proceedings of ASME 2007, Keystone, Colorado July 20-24/2007.

M. Ionita, PhD Thesis, Department of Bioengineering, Politecnico di Milano, 2008.

**Prospect for further use:**

During the project the knowledge generated has been sufficient to now extend the investigations systematically to other materials and to combine them with respective experimental studies. The aim is to now routinely utilize CAMD as a tool for the development of new biomaterials with tailored properties.

**Task 7.2.1:** CADM effort for the design of bulk and interface models of copolymers also with different amount of additives (from 10 to 70% of additives). The models have been investigated concerning the diffusion gases and of water molecules in the polymer matrix and the influence on transport in function of different additives.

**Description of background and key results**

The main second goal of WP7 has been the simulation of various penetrants transport through such polymers filled by suitable additives in order to reduce the plasticization effect of water or condensable gases (e.g CO<sub>2</sub>) and precursor of biomolecules of pharmaceutical interest. Vapour and gas transport through polymeric films is of great interest for different industrial fields. There membrane

processes are potentially extremely competitive with alternative technologies, e.g. for separation of polarizable/nonpolar gas pairs such as H<sub>2</sub>O/ N<sub>2</sub> or CO<sub>2</sub>/CH<sub>4</sub>. The high performance in terms of vapour and condensable gases transport is typical of block poly(ether/amide). The performance of membranes derived from such copolymers has been improved [A. Gugliuzza, E. Drioli, *Polymer Journal*, 44/7 2003 2149; T. Miyata, Y. Nakanishi, T. Uragami, *Macromolecules*, 1997, 30, 5563] in terms of vapour/gas transport and processability by blending the polymer matrix with suitable additives at low molecular weight. When adding organic molecules with different chemical structure to a polymer matrix, the system morphology, the chemical composition and even the physico-chemical properties change, influencing the transport through the membranes. For this reason the understanding of the gas and vapour permeation mechanism and the evaluation of the additive effects achieve large interest. In this workpackage bulk models of pure copolymers and of copolymers containing additives in various concentration have been used to study gas and vapour transport properties. Also models for interfaces between e.g. a water phase and a polymer surface to analyse the surface tension have been prepared. In order to assess possible relationships between their chemical structure and their macroscopic physico-chemical properties copolymer based materials have been studied at the molecular level by means of computational models based on quantum mechanical (QM) and molecular dynamics (MD) level. The computational activity has been closely linked to the experimental one performed at WP2. Bulk amorphous 3D periodic cells of the pure PEBAX 2533 have been analysed in terms of the permeation behavior of six permanent gases, N<sub>2</sub>, O<sub>2</sub>, CH<sub>4</sub>, He, H<sub>2</sub> and and to identify the role played by the soft ether block (PTMO) in gas permeability.

Gas1/ Gas2	S(Gas1)/S(Gas2)			
	Exp.	Exp. <sup>a</sup>	TST	GCMC
O <sub>2</sub> /N <sub>2</sub>	4.0	4.6	3.75	3.1
CH <sub>4</sub> /N <sub>2</sub>	1.39	2.0	2.12	4.5
CO <sub>2</sub> /N <sub>2</sub>	23.6	28.8	14.9	6.0
CO <sub>2</sub> /H <sub>2</sub>	51.5	43	38.2	32.5

Table 1 - Solubility selectivity for several gas pairs in PEBAX<sup>®</sup>2533 at 25°C. <sup>a</sup>At 35°C (V. I. Bondar, B. D. Freeman, I. Pinnau, *J Polym. Sci. Part B: Polym. Phys.* 37 (1999) 2463-2475)

The transport of this single species through Pebax membranes is strongly affected by its low solubility in the polymer matrix as compared with a more polar and condensable gas such as CO<sub>2</sub>. In this case, the contribution of the diffusivity is overshadowed by its limited affinity to the segment chains. The best selectivities of these membranes were estimated for polar/nonpolar pair of penetrants such as CO<sub>2</sub>/H<sub>2</sub> and CO<sub>2</sub>/N<sub>2</sub> as shown in Table 1, confirming the better performance of this class of poly(ether-b-amide) block co-polymers than that of conventional rubbery polymers. The predominance of the solubility contribution appears, therefore, to be the driving force of the selective process. The fundamental contribution to the transport of CO<sub>2</sub> in PTMO80/PA20 is given by the solubility, i.e. the interaction between the gas and the polymer matrix. The soft block of the copolymer (PTMO) plays the main role in the solubility of CO<sub>2</sub> in PEBAX<sup>®</sup>2533. In order to explain the high CO<sub>2</sub> solubility, were investigated associations between CO<sub>2</sub> and possible sites of interactions of the polymeric chains. Nitrogen atoms of amide groups, carboxylic groups and ester linkages in PEBAX<sup>®</sup>2533 and oxygen atoms of PTMO have been explored by the radial distribution function  $g(r)$  (RDF). The RDF analysis is defined as the probability of finding an atom at distance  $r$  from another atom compared to the ideal gas distribution. The calculated radial distribution functions, averaged over all atom pairs are plotted in Figure 1. Results indicates a strong association (a large peak between 2.5

and 6.75 Å) between CO<sub>2</sub> and the oxygen atoms of polyether (PTMO). The association effect is weakened at positions along the amidic component of the chain, resulting in a lower contribution of the hard segments to the quadrupolar CO<sub>2</sub>

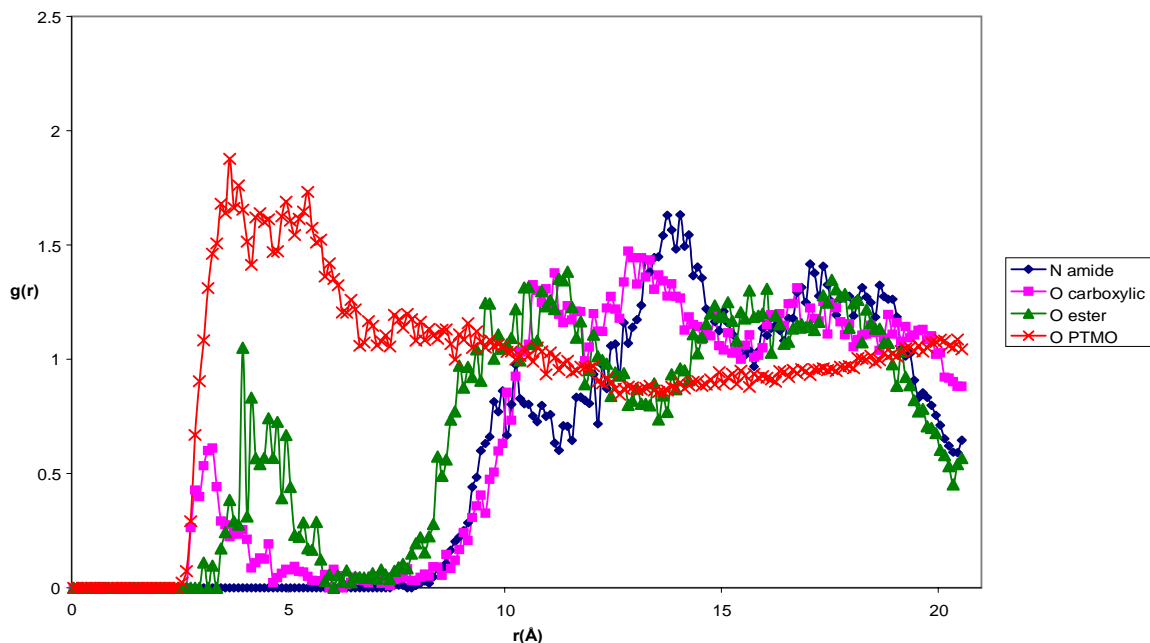


Figure 1 Plot of the pair correlation function,  $g_{ij}(r)$  versus the separation distance,  $r(\text{Å})$ , between CO<sub>2</sub> and the oxygen atoms of PTMO, the nitrogen atoms of amide groups, carboxylic groups, and ester linkages, of the side chains of PEBAX.

**Task 7.2.2:** The systematic molecular dynamics simulation of bulk and interface models constructed in Task 7.2.1. Quantum mechanical calculations to have better insights on the elementary interactions between water/small penetrants and the polymeric matrix.

#### Description of background and key results

Atomistic models were implemented and refined for Pebax with different amount of *o/p*-N-ethyl-*p*-toluensulphonamide (KET), respectively with copolymer-additive weight ratio of 90:10, 70:30, 50:50, 40:60. Each bulk model consisted of a periodic cubic box with a size dimension of about 40 Å, containing about 7600 atoms. After the equilibration procedure the permeability properties were investigated analysing the MD-NVT dynamics run of the inserted small molecules of water. For all boxes MD simulation have been performed for 1,5 ns with a 1 fs timestep. Interface models of pure Pebax and with 30% of KET have been built and assembled with a layer of water molecules by using the build layer module of the Accelrys software. Long dynamics NVT for the analysis of the water interaction with the polymer matrix have been performed. Then a multidisciplinary approach, i.e. using experimental infrared analysis, MD simulation and QM calculations, was used for establishing the mechanism controlling the water sorption in modified Pebax membranes.

Experimentally, an increase in water uptake was estimated up to modifier content of 50 wt.%. Further slight increase in concentration produced dramatic decrease in water dissolution. As largely confirmed by infrared analysis and surface energy properties, the decrease in water affinity of the polymer matrix was ascribed to the accessibility and availability of the polar head of the modifier. The chemical group accessibility and availability has been attributed to both the changes in polymer packing and to direct intermolecular interactions involving modifier molecules, respectively.

Molecular dynamic simulations yielded indication about the modifier distribution into the polymer membranes by evaluating the polymer-modifier as well as the modifier-modifier distances. Then density functional electronic structure calculations have been performed on of the most stable water-modifier geometries obtained via MD simulation. The MD and QC calculations have shown that the interaction energy between water and modifiers decreased, as modifier dimers are formed. This phenomenon is thought to occur at high concentration of the modifiers. No variations in the dipole moments of water-dimers structures were found with respect to the single KET. Consequently, due to

water-dimer complexes, the number dipole moment does not change with increasing modifier concentrations and possible effects on the polymer chain polarization should be not expected. The key indication derived from theoretical analysis highlighted the geometries involving two linked modifiers, establishing the intermolecular interaction N-H...O-S-O, underlying the polymer influence on this interaction. This information has been of significant importance, because it explains how a second water molecule interacts lesser with  $[\text{H}_2\text{O}\cdots(o\text{-KET})_2]$  complex than a separate  $o\text{-KET}$ . The analysis of polymer-water-monomer-water-monomer has been performed by using a restraint to simulate the polymer matrix. These restrains at QC level have been obtained by defining a harmonic constraint (spring) along the length of the N-H...O-S-O bond. The effects of the polymeric chains appeared significantly decisive: in this case the second water molecule preferred to bind the oxygen of the free sulphonamide moiety (**II**) instead to break the N-H...O-S-O bond between the modifiers **I** and **II** (Figure 2).

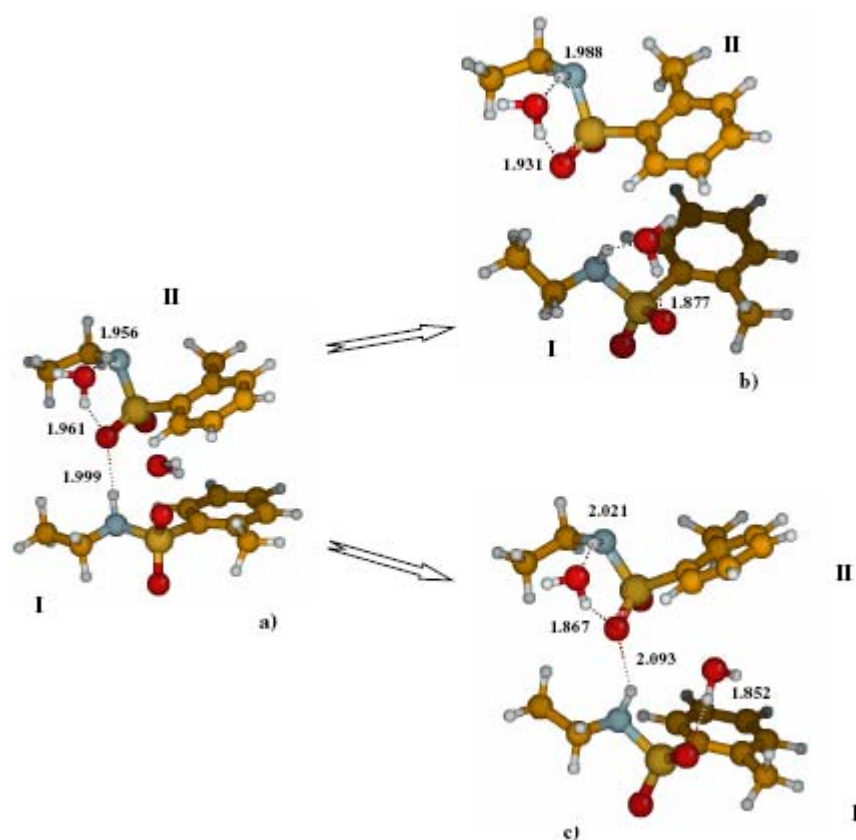


Figure 2. Starting geometry of  $[(\text{H}_2\text{O})\cdots(o\text{-KET})_2]$  complex and a second water molecule (a). Density functional minima of  $[(\text{H}_2\text{O})_2\cdots(o\text{-KET})_2]$  without (b) and with constrain (c). Acceptor and donor hydrogen distances were reported and expressed in Angstroms Å

In addition, the dipole moments of  $[\text{H}_2\text{O}\cdots(o\text{-KET})_2]$  and  $[(\text{H}_2\text{O})_2\cdots(o\text{-KET})_2]$  complexes are almost equal to the dipole moment of the  $o\text{-KET}$  and  $[\text{H}_2\text{O}\cdots(o\text{-KET})]$ . This means that the increase in modifier molecule number does not produce a corresponding increase in the overall dipole moment and consequently in the polymer polarization.

#### Publications submitted so far:

1. L. De Lorenzo, Molecular dynamic simulations of gas transport properties of poly(amide-12-b-ethylene oxide) copolymers, ., Proceedings of NYM8 Network Young Membrains, Rende (Italy), 21-23/09/2006

2. A. Gugliuzza, G. De Luca, E. Tocci, L. De Lorenzo, E. Drioli, “ Experimental and theoretical evaluation of the membrane affinity to water: role of modifiers in the control of the matrix performance” *Desalination* 2006, 200: 256-258
3. E. Drioli, New self-assembled block co-polyamide membranes: key factors in the control of the transport, oral presentation XXIII EMS Summer School on Membranes, Prague, 3-6 /09/2006
4. A. Gugliuzza, G. De Luca, E. Tocci, L. De Lorenzo, E. Drioli, Intermolecular interactions as controlling factor for water sorption into polymer membranes, *J. Phys. Chem. B* **2007**, *111*, 8868-8878
5. E. Tocci, A. Gugliuzza, L. De Lorenzo, M. Macchione, G. De Luca, E. Drioli, Transport properties of a co-poly(amide-12-b-ethylene oxide) membrane: a comparative study between experimental and molecular modelling results, 2008 *submitted*

**Prospect for further use:**

The results obtained during the project, in relation to the understanding of the vapour/gas permeation mechanism, the evaluation of the temperature and additive effects transport through such polymers filled by suitable additives, in combination with experimental studies are quite satisfactory. The aim is to employ CAMD techniques as a tool for the design of polymeric materials for separation of polarizable/nonpolar gas properties.

**WP8 “Statistical Interface to the CULGI software package”:** This workpackage aims at the development, validation and dissemination of the Statistical Interface to Mesodyn BV’s proprietary CULGI software package, a computer package for the statistical database handling and modelling of soft materials, through interfacing QSAR with mesoscopic and molecular modelling and Neural Networks. There are good indications that adapting the Neural Network strategy, in combination with mesoscopic and nanoscopic modelling will lead to breakthroughs in technology, and commercialisation of soft materials.

In the course of the Multimatdesign project, Culgi BV developed into an international computational chemistry company dedicated to providing industry with revolutionary modelling tools for the rational design of soft matter formulations. Culgi employs computational scientists, physical chemists, and software engineers, who aim to boost the research and development in soft matter formulations and help find solutions to industrial problems. In 2008, Culgi has 15 employees, up from 2 at the start of the Multimatdesign project, with offices in Europe (main office in Leiden, The Netherlands), and subsidiaries in USA and China.

Culgi develops and markets the Culgi multiscale modeling library, and offers scientific support and consulting through a network of application scientists.

Computer modelling is a valuable tool for efficient formulation development in such diverse industries as chemicals, petroleum, pharmaceuticals, automotive, aerospace, and home & personal care. Integrating modelling activities into the R&D process increases the rate at which new products can be brought to market. A number of modelling techniques, ranging from atomistic simulation to field based mesoscopic models, to statistical methods are used to solve various problems in the research process.

In the Multimatdesign project, we developed a theory or a hybrid between Support-Vector Machine and Mesoscopic Modelling (first year), and developed the Culgi library.

Also in this first first year of Multimatdesign, as a result of many discussions with industry (amongst others, Air Liquide), we firmly established the following business model:

- Commitment to a “professional-to-professional” model. PhD level scientists at Culgi work directly with clients to ensure that the modelling software suits their needs. Because we develop our software internally we are exceptionally responsive to customer needs.
- Proprietary code development. Through both graphical and script-based interfaces, users have great flexibility in working with the Culgi library.
- A fully integrated simulation and modelling framework. By developing all simulation techniques in a single environment, Culgi makes it easy to do true multiscale modelling. This includes both novel hybrid modelling techniques and tools to pass information between simulations at different scales.

The Culgi Library is a multi-functional chemistry simulation platform for soft matter research, providing modelling and simulation algorithms covering a range of length and time scales. A unique aspect of the library is that it enables novel hybrid calculations that are proprietary to Culgi, such as dissipative particle dynamics with bond interactions and Poisson-Boltzmann electrostatics, embedded particle hybrid bead-field simulation methods, mappers between mesoscopic and molecular models, mesoscopic computational fluid dynamics, and mesoscopic reaction models.

The Culgi Library is a professional object-oriented C++ scientific library. It includes modeling, calculation, visualization, and analysis engines. It provides interfaces to customers in a user-friendly style. The library is designed for a range of users from the laboratory chemist to the experienced numerical modeler. Therefore, Culgi provides multiple interfaces for working with the library. The Culgi Graphical Programming Environment (GPE) provides an easy to learn entry point in which a user can quickly develop sophisticated simulation scripts via a graphical, menu based interface. For users with more programming experience, who prefer the flexibility of writing and maintaining their own code, we provide the option of accessing the library through Python or Tcl scripts, as well as C++.

The Culgi multiscale modelling library provides solutions for researchers in industries such chemicals, petroleum, pharmaceuticals, automotive, aerospace, and home & personal care. The list of industrial sectors that the Culgi library covers is much broader than the original polymer membrane modeling task anticipated in Multimatdesign. The broadening of scope is very favourable for dissemination of Multimatdesign results, and it demonstrates the strength of the developing methods of Culgi. The industry that is currently covered by the library includes:

#### Chemicals

Companies throughout the chemicals industry recognize the need to efficiently develop new chemicals and formulations, whether the end goal is to improve the feel of a cosmetic, the performance of a polymer, or the viscosity index of a lubricant. The development of new products must be streamlined and modelling provides a cost-effective screening tool to reduce time to market. Culgi is involved in several projects, such as modeling efficient polymer processing, and adhesives modeling.

#### Pharmaceuticals

The pharmaceutical industries face the challenge of drugs of low solubility (Class III and IV), that need to be formulated very carefully, for example as colloidal dispersion or through a slow release polymer matrix. Culgi is involved in designing such formulations by a variety of modeling techniques. Increasingly, the library is also being used in the biological domain, for example in the screening of multiblock cationic peptides for membrane fusion.

#### Automotive/Aerospace

Research in the automotive and aerospace industries focuses on a number of issues. These include lightweight materials with the desired mechanical properties, efficient fuel cells,

coatings, and reduction of wear and fatigue of vehicular components. Culgi is currently involved in the development of novel polymer nanocomposites for automotive parts, in the new Framework 7 Nanomodel project, in collaboration with several industries (Fiat, Bosch, BASF) and universities (amongst others, the group of professor Theodorou, partner in Multimadesign)

#### Home & Personal Care

The rapid development of new products plays a key role in growth for the personal care and consumer product industries. In areas such as detergents, skin and hair care, and household cleaning materials, competitive advantage derives from the optimization of formulations for desired properties and increased shelf life. Culgi is involved in a number of such projects, for example in the study of long term stability of multicomponent detergent mixtures.

#### Petroleum

Major challenges in the petroleum industries include the efficient extraction of petroleum from a variety of sources, and viscosity lowering of crude oils for transport. Current work at Culgi focuses on the use of surfactant emulsion technology to enhance oil recovery and transport processes. Additional topics of interest include refining and downstream processes.

An illustrative example of the multiscale modeling is in the figure [Culgi demo], that shows both a hybrid mesoscopic model of a detergent mixture, including charged colloids, polymer and surfactants, and also a molecular model, generated with the meso-molecular mapper functionality.

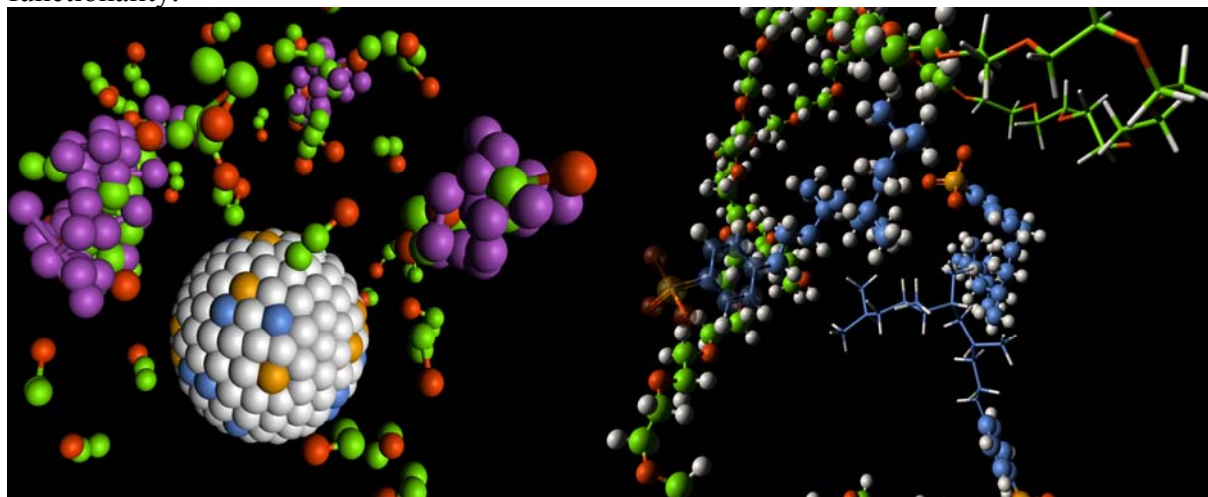


Figure [Culgi Demo]. Illustrative example of Culgi Library functionality developed in Multimadesign. On the left is a coarse-grained model of a complex detergent mixture, with a charged colloidal particle, polymers and charged surfactants. All species interact dynamically through a Dissipative Particle Dynamics model, with Poisson-Boltzmann interaction for the charges. The polymers and surfactants are modeled as flexible strings of beads, but the colloid has fixed internal bead positions, i.e. it is a solid particle. From this coarse-grained model, a fine-grained molecular model (on the right) is generated by a Mapper calculation, that warps (part of the) mesoscopic model to molecular detail. Calculations on the mapped molecular model are with Molecular Dynamics, using the OPLS forcefield. Solvent molecules and electrostatic fields are omitted for clarity.

## **2. Dissemination and use**

### **Publishable results**

#### **New polymer for membrane separation of gaseous mixtures**

The polymer of this patent is recommended as material for gas separation membrane distinguished by high permeability and solubility controlled permeation. Hence, it can be useful for separation of hydrocarbon mixtures, e.g. natural or associated petroleum gas. Advantage of this polymer is that at pressure of 1 atm or higher permeability coefficients of heavier hydrocarbons (e.g. butane) is greater than that of methane. Therefore, hydrocarbons C3+ are accumulated in permeate. The advantage of this polymer as membrane material as compared to polytrimethylsilylpropyne is that it does not undergo rapid aging.

Possible market applications include treatment of natural or associated petroleum gases. Also an application as membranes in membrane contactors can be envisaged: separation of CO2 from natural gas (sweetening of natural gas). This possibility is tested now in another project of EC: 7FP project with Dutch and Russian participants.

This technology is currently at the laboratory prototype stage. As above, potential collaboration is through another 7FP project.

Patent number RU2296773

Contact details: [Yampol@ips.ac.r](mailto:Yampol@ips.ac.r)

### **Hybrid mesoscopic simulation method**

A new hybrid mixed particle/field mesoscopic simulation method is implemented in the commercial Culgi simulation package as a module. This Culgi package is script-based and flexible, and facilitates a wide range of methodologies at various levels of description, as well as routines for IO, visualisation, characterisation and converters. Culgi is currently used for computational research in academic groups and chemical industry (consultancy). In contrast to most mesoscopic methods, which are based on a single (particle or field) description of constituents, the hybrid method increases the ability to include heterogeneity by allowing for a description of constituents in particles and/or fields in one simulation volume. A conceptual description was published, and couples the dynamic density functional (field) theory with Brownian (particle) dynamics. The Culgi hybrid module is fully operational, but further validation by intricate experiments is required. The new functionality will be exploited to model polymer nanocomposite systems (within the NanoSci-E+ collaborative framework).

Publication: G.J.A. Sevink and J.G.E.M. Fraaije, Modeling complex systems in full detail: a new approach. In: AIP Proceedings 982 (Eds. M. Tokuyama, I. Oppenheim, H. Nishiyama) 491-497, 2008.

Contact details: <http://www.culgi.com>

### **Summary table about dissemination**

<b>Year</b>	<b>Written publications</b>	<b>Oral presentations</b>
<b>1</b>	<b>13</b>	<b>46</b>
<b>2</b>	<b>38</b>	<b>67</b>
<b>3</b>	<b>23</b>	<b>40</b>